High-affinity iron and calcium transport pathways are involved in U(VI) uptake in the budding yeast Saccharomyces cerevisiae

Benoît Revel, Patrice Catty, Stéphane Ravanel, Jacques Bourguignon, Claude Alban

High-affinity iron and calcium transport pathways are involved in U(VI) uptake in the budding yeast *Saccharomyces cerevisiae*

Benoît REVEL[1], Patrice CATTY[2], Stéphane RAVANEL[1], Jacques BOURGUIGNON[1] and Claude ALBAN[1]

[1]Univ. Grenoble Alpes, CEA, INRAE, CNRS, IRIG, LPCV, 38000 Grenoble, France

[2]Univ. Grenoble Alpes, CEA, CNRS, IRIG, LCBM, 38000 Grenoble, France

Correspondence:

claude.alban@cea.fr

Univ. Grenoble Alpes, INRAE, CEA, CNRS, IRIG, LPCV, 38000 Grenoble, France

jacques.bourguignon@cea.fr

Univ. Grenoble Alpes, CEA, INRAE, CNRS, IRIG, LPCV, 38000 Grenoble, France

Keywords: Yeast, radionuclide, uranium, metal, incorporation, accumulation, mutants

Highlights

- Living yeast *Saccharomyces cerevisiae* is able to take up U
- Availability of a metabolizable substrate stimulates U uptake
- Calcium, iron and copper inhibit U uptake
- Strains deleted in Mid1/Cch1 calcium channel and Ftr1 iron permease are affected in U uptake
- Expression of *MID1* gene in *mid1Δ* strain restore wild type levels of U uptake

Abstract

Uranium (U) is a naturally-occurring radionuclide toxic for living organisms that can take it up. To date, the mechanisms of U uptake are far from being understood. Here, we used the yeast *Saccharomyces cerevisiae* as a unicellular eukaryote model to identify U assimilation pathways. Thus, we have identified, for the first time, transport machineries capable of transporting U in a living organism. First, we evidenced a metabolism-dependent U transport in yeast. Then, competition experiments with essential metals allowed us to identify calcium, iron and copper entry pathways as potential routes for U uptake. The analysis of various metal transport mutants revealed that *mid1Δ*, *cch1Δ* and *ftr1Δ* mutants, affected in calcium (Mid1/Cch1 channel) and Fe(III) (Ftr1/Fet3 complex) transport, respectively, exhibited highly reduced U uptake rates and accumulation, demonstrating the implication of these import systems in U uptake. Finally, expression of the *Mid1* gene into the *mid1Δ* mutant restored U uptake levels of the wild type strain, underscoring the central role of the Mid1/Cch1 calcium channel in U absorption process in yeast. Our results also open up the opportunity for rapid screening of U-transporter candidates by functional expression in yeast, before their validation in more complex higher eukaryote model systems.

Introduction

Uranium (U) is a naturally-occurring trace metal element and radionuclide ubiquitous in the Earth crust. It is primarily redistributed in the environment by anthropogenic activities related to U mining and milling industries, civil and nuclear activities, and extensive enrichment of agricultural soils with phosphate fertilizers, which may be significantly contaminated with U. The accumulation of U in soil, water and air can pose potential risks to ecosystems, agrosystems, and ultimately human health through food chain contamination, as the radionuclide has both chemical and radiological effects. Natural U is of low radiotoxicity due to its isotopic composition (>99% ^{238}U) but the uranyl cation (UO_2^{2+}) that is prevalent in oxidizing environments is highly chemotoxic (Gao et al., 2019; Ribera et al., 1996). Since U is not an essential element, its uptake and intracellular trafficking depends on existing metal transporters or channels of broad metal selectivity. In particular, cation transporters offer potential transport pathways for toxic metals. These transport systems may differ from a living organism to another. Even if U is known for a long time to interfere with iron, manganese, phosphate and calcium homeostasis in microorganisms, plants and animals, and despite significant efforts to decipher the mechanisms that contribute to the absorption of the radionuclide from the environment, no U entry route in the cell has been identified so far in prokaryotic or eukaryotic cells (Berthet et al., 2018; Gao et al., 2019; Khare et al., 2020) and references therein).

The yeast *Saccharomyces cerevisiae* has long been used as a powerful eukaryotic cell model for studying cell transport systems, in particular those related to trace elements transport and homeostasis (Eide et al., 2005). The usefulness of yeast for genome-wide studies of nutrient homeostasis markedly increased with the completion of the Saccharomyces Genome Deletion Project that resulted in a collection of mutant strains disrupted in most of the approximately 6,000 genes in the yeast genome (Winzeler et al., 1999). This strain collection provides a unique resource for the analysis of gene function in a eukaryotic cell. Moreover, insights from yeast can be easily translated to other organisms, making it an efficient and attractive model system. In many instances, for example, it has been shown that mammalian proteins are capable of functionally replacing yeast proteins, thereby revealing their remarkable functional conservation. Thus, yeast has allowed the identification and molecular understanding of human transporters and has provided insights into diseases that result from defects in ion

homeostasis (Cyert and Philpott, 2013; Laliberté and Labbé, 2008; Van Ho et al., 2002). Functional expression of plant genes in yeast also enabled the identification of numerous plant ion transporters before their validation and further characterization *in planta*. This includes, but is not restricted to, the wheat potassium transporter HKT1 (Schachtman and Schroeder, 1994), the Arabidopsis iron transporters IRT1 (Eide et al., 1996), NRAMP1 (Curie et al., 2000), NRAMP3 and NRAMP4 (Thomine et al., 2000), the Arabidopsis MCA1 and MCA2 calcium channels (Nakagawa et al., 2007; Yamanaka et al., 2010) and the Arabidopsis copper transporter COPT1 (Kushnir, 1995). Finally, a systematic approach for transforming yeast into metal hyperaccumulators was recently designed (Sun et al., 2019). This work demonstrated that yeast can be engineered to hyperaccumulate metals by overexpressing and evolving native metal transporters and engineering mechanisms for metal detoxification, allowing to consider the use of this organism as an integral tool for waste treatment processes and recycling.

In this study, we used *S. cerevisiae* to identify pathways for U entry into an eukaryotic cell. U has a strong propensity of biosorption to dead or living yeast cell wall, a process that do not depend on temperature and that has been studied in a bioremediation context (Lu et al., 2013; Shen et al., 2018). Very few studies, however, report on U uptake by yeast cells (Kolhe et al., 2020; Ohnuki et al., 2005; Volesky and May-Phillips, 1995). Here, we developed an efficient and sensitive assay for measuring U uptake in yeast that discriminates U adsorbed on cell surface from internalized U. Uranium uptake was shown to depend on cell metabolism. By using a combination of competition experiments with metal ions and the analysis of metal transport deficient mutants, we showed that calcium, iron and copper assimilation pathways are important routes for U uptake. More precisely, we demonstrated that the high-affinity calcium channel Mid1/Cch1 and the high-affinity iron transporter Ftr1/Fet3 complex are major U importers in *S. cerevisiae*. The potential use of yeast mutants for these transport systems as tools to investigate candidate mammalian and plant U transporters by functional expression, for future human health, phytoremediation and food chain management purposes is discussed.

Materials and Methods

Strains and plasmids

Table I lists all yeast strains employed in this study, which were derived from the wild-type *S. cerevisiae* strain BY4742 (MATα, *his3Δ1, leu2Δ0, lys2Δ0, ura3Δ0*) (Brachmann et al., 1998) and were generated by the Genome Deletion Project (Winzeler et al., 1999). All strains were obtained from EUROSCARF.

Low copy number plasmid YCpMID1 [*URA3 MID1 ARS1 CEN4 amp*^{r}] (Iida et al., 2004) was kindly provided by Professor Iida (Tokyo Gakygei University). Empty low copy number plasmid pRS316 [*URA3 ARSH4 CEN6 amp*^{r}] (Sikorski and Hieter, 1989) was used as control. High copy number plasmids YEp351-FTR1-myc [*LEU2 FTR1-myc 2 µm-ori amp*^{r}], YEp352-FET3-HA [*URA3 FET3-HA 2 µm-ori amp*^{r}] and corresponding control empty plasmids YEp351 [*LEU2 2 µm-ori amp*^{r}] and YEp352 [*URA3 2 µm-ori amp*^{r}] (Stearman et al., 1996) were kindly provided by Doctor Stearman (Indiana University). Plasmids were introduced into yeast strains by using conventional lithium acetate transformation procedure (Kuo and Campbell, 1983). The *Escherichia coli* strain DH5α was used for plasmid amplifications.

Growth media and culture conditions

Yeast strains were cultured to late-exponential growth phase at 30°C, under continuous stirring at 200 rpm, either in YD medium (10 g/l yeast extract, 20 g/l glucose) or, where indicated, in YG medium (10 g/l yeast extract, 20 ml/l glycerol). Transformed cells were cultured in modified synthetic media SD/Ca100 or SD/Fe0 (6.8 g/l Yeast Nitrogen Base without amino acids; Foremedium Ltd, containing 100 µM $CaCl_2$ instead of 900 µM $CaCl_2$ or 0 µM $FeCl_3$ instead of 1 µM $FeCl_3$ in standard mixture, and 20 g/l glucose), supplemented with appropriate amino acids plus adenine (by addition of 0.77 g/l of Complete Supplement Mixture Drop-out formulation minus leucine and/or minus uracil; MPBio). Cells were counted using a LUNA-FL automated cell counter (Logos Biosystems).

Kinetics of U uptake and accumulation

Cultured yeast cells were harvested by centrifugation at 4000 g for 5 min, washed twice with water and resuspended in 10 mM 2-(N-morpholino)ethanesulfonic acid (MES), pH 5.5 buffer, at a concentration of 2 X 10^8 cells/ml with or without a carbon source (20

mM glucose, or 3% (v/v) glycerol when cells were grown in YG medium). After a 15 min preincubation at 4°C (in a cold room) or 30°C in a Xtemp climatic chamber (Mechanical Convection Oven XT5116 – IN140) with 30 rpm rotary shaking, uranyl nitrate ($UO_2(NO_3)_2.6H_2O$; >98%; Fluka) was added to 10 ml of the cell suspensions to the desired final concentration, from convenient stock solutions. At appropriate intervals, samples (0.5 to 1 ml) were taken and centrifuged at 14 000 g for 2 min. Cell pellets were then washed twice with 1ml 10 mM sodium carbonate. NaN_3 inhibitor or other metals used in competition experiments were added in the uptake assay at the beginning of the preincubation period. Cell-free controls were conducted using the same procedure to assure that the amount of U precipitating in the reaction medium or adsorbed on the tube wall was negligible under our assay conditions, confirming that U removal resulted exclusively from biotic interaction.

Determination of cell viability

Yeast viability kit based on fluorescein diacetate/propidium iodide staining method was used to analyze the cell concentration and viability of yeast samples with the automated fluorescence cell counter LUNA-FL, following the manufacturer's recommendations (Logos Biosystems). In all experiments performed in this study it was found that cell viability was not significantly affected at the end of the absorption kinetics of U (Supplemental Figure 1 A-D).

U quantification by inductively coupled plasma-mass spectrometry (ICP-MS)

Yeast cells were digested at 90°C for 4 hours in 65% (w/v) HNO_3 (Suprapur, Merck). Mineralized samples were diluted in 0.5% (v/v) HNO_3 and analyzed using an iCAP RQ quadrupole mass instrument (Thermo Fisher Scientific GmbH, Germany) equipped with a MicroMist U-Series glass concentric nebulizer, a quartz spray chamber cooled at 3°C, a Qnova quartz torch, a nickel sample cone, a nickel skimmer cone with a high-sensitivity insert, and an ASX-560 autosampler (Teledyne CETAC Technologies, USA). ^{238}U was analyzed using the standard mode. Concentrations were determined using standard curves prepared from serial dilutions of $UO_2(NO_3)_2$ and corrected using an internal standard solution containing ^{172}Yb added online. Data integration was done using the Qtegra software (Thermo Fisher Scientific GmbH, Germany).

Statistical analyses

Statistical parameters including the definitions and values of n and SDs are reported in the figures and corresponding figure legends. Non-parametric statistical analysis was performed on data sets analyzed in Fig. 4, 6 and 7, which typically contain small sample sizes (n<10) and do not meet the assumptions of parametric tests (normal distribution and homogeneity of variance, as determined using the Shapiro-Wilk and Fisher tests, respectively). When reporting significance, multiple non-parametric comparisons were performed with the Dunnett's many-to-one test using the package nparcomp (Konietschke et al., 2015) and the R computing environment (R Development Core Team, 2011). The normal approximation option was used and the confidence level was set at 99.9 %.

Results

S. cerevisiae is able to take up U

The budding yeast *S. cerevisiae* is known to adsorb large amounts of U at the cell surface. This massive adsorption of U possibly hides a potential U uptake whose existence and *a fortiori* mechanisms are still largely unknown. To analyze the capacity of yeast cells to transport U intracellularly, we measured kinetics of U incorporation by the strain BY4742 at different U concentrations and two different temperatures. In a first set of experiments, yeast cells (2×10^8 cells/ml) were challenged with 10 µM uranyl nitrate in 10 mM MES buffer pH 5.5 in the presence of 20 mM glucose for up to 3 h, at 4°C or 30°C. Cellular U content was measured by ICP-MS after two washing steps with 10 mM sodium carbonate. As shown in Figure 1, more than 70% of U initially added to the reaction medium was recovered immediately in the unwashed cell pellets (time 0 corresponds to the time necessary to separate cells from surrounding buffer by centrifugation after U exposure, *i.e.* less than 5 min). This fast and temperature independent U binding to yeast cells corresponded to adsorption. Indeed, metal cations adsorption on yeast cell wall is reported to be unchanged across the temperature range 4-30°C (Blackwell et al., 1995; White and Gadd, 1987). At 4°C, the level of biosorbed U remained stable throughout the kinetics. After one washing step with sodium carbonate most of U adsorbed at the cell surface was washed out and recovered in the washing solution after centrifugation (Figure 1A). After the second washing step, almost all adsorbed U was eliminated (U measured in cell pellets did not exceed the background value throughout the kinetics, demonstrating the efficiency of

the washing procedure). This demonstrated that almost no U enters yeast cells at 4°C. At 30°C, U associated to the cell pellets was only partially washed away with sodium carbonate. Indeed, a time-dependent increase of U incorporated was observed in washed cells (starting from nearly 0 immediately upon addition of U), which correlated with a decrease of U remaining in the incubation medium and in the washing solutions (Figure 1B). Under these experimental conditions, we measured a rate of 70-100 ng U (0.29-0.42 nmol) transported per hour by 10^8 cells. Altogether, these experiments showed that yeast cells are able to incorporate intracellularly in a temperature dependent manner a portion of U added exogenously after a rapid and massive adsorption at the cell surface.

U transport in *S. cerevisiae* requires an active metabolism

To learn more about U transport mechanisms in *S. cerevisiae*, the effect of energy source on U uptake was investigated. To this aim, cultured cells suspended in MES buffer were challenged at 30°C and 4°C with increasing amounts of uranium nitrate from 1 to 10 µM either in the presence or absence of glucose for up to 24h. As already suggested by experiments depicted in Figure 1, a huge difference in U uptake was observed between 30°C and 4°C (Figure 2). At 30°C, an important dose-dependent U influx was observed in the presence of glucose. Under these conditions, U uptake was linear for at least 3h for all U concentrations tested and after 24 h incubation, 30% to 40% of U initially present in the reaction mixture accumulated into the cells (Figure 2). In the absence of glucose, accumulation levels of U were much lower. Interestingly, the ratio between the glucose-dependent and the glucose-independent U accumulation increased with U concentration (ratio around 2 at 1 and 3 µM U (Figure 2A,B); ratio of 6 at 10 µM U (Figure 2C)). U uptake measured at 4°C was very low, but for the three U concentrations tested, a positive effect of the presence of glucose on U uptake was also observed. The transport rate of U was assessed in the presence of glucose at 30°C on 90 min kinetics. As shown in Figure 3, an apparent V_{max} of 145±5 ng (0.6 nmol) U incorporated per hour by 10^8 cells was reached at saturated concentrations above 50 µM and an apparent K_m for U uptake of 9.0±1.4 µM was calculated from the Michaelis Menten equation (Figure 3). Note that cell viability was checked throughout the experiment and was found to be largely unaffected regardless of the tested condition (Supplemental Figure 1A). The stimulation of U uptake in the

presence of glucose might be attributable to metabolism-dependent intracellular U accumulation. The requirement of an active metabolism was also checked using glycerol, an alternate but non-fermentable carbon source, and sodium azide, an inhibitor of the mitochondrial respiratory chain. As shown in Figure 4, similar U transport rates were measured in the presence of glycerol and glucose in the absence of sodium azide. The latter almost completely abolished U uptake, regardless of the energy source used in the assay. Altogether, these results demonstrate that U transport within yeast cells is essentially a metabolism-dependent process that requires a functional respiratory chain able to produce ATP.

Fe^{2+}, Fe^{3+}, Cu^{2+} and Ca^{2+} compete with U for transport in *S. cerevisiae*

As a first step toward the identification of U uptake pathways in yeast, its accumulation was measured in the presence of various essential metals whose transport systems are well described. Indeed, since U is not essential for any living organism, its uptake probably depends, at least in part, on these transport systems that, taken together, display a broad metal selectivity, including toxic metals (Cyert and Philpott, 2013; Van Ho et al., 2002). In these competition experiments, U uptake (from 10 µM uranyl nitrate) was challenged with nine essential metals (Fe(III), Cu(II), Fe(II), Ca(II), Mo(VI), Mn(II), Zn(II) Co(II) and Mg(II)) at concentrations varying from 10 µM to 1 mM.

As shown in Figure 5, three metals, namely copper, iron and calcium competed with U uptake. $CuSO_4$ (Figure 5A) and $FeCl_3$ (Figure 5B) displayed the strongest concentration-dependent inhibitory effect. At 10 µM, both metals had no or limited effect on U uptake. At 50 µM, they caused a 2- and 3-fold reduction of U accumulation after 4h, respectively. The inhibitory effect of these two metal ions was even more marked at 100 µM with a 4-fold reduction of U accumulation after 4 h. If we consider the initial rate of U transport as measured over the first 90 min (see also Figures 2 and 3), it turns out that the low accumulation of U in the presence of Cu(II) and Fe(III) likely came from a reduction in the initial rate of U uptake. The inhibitory effects of Ca(II) (Figure 5C) and Fe(II) (Figure 5D) were different from those of Cu(II) and Fe(III) in our competition assays. They were globally lower and observed at higher concentrations. Indeed, 1 mM of $CaCl_2$ or $FeSO_4$ were required to induce a nearly 2-fold reduction of U uptake at 4h. Remarkably, Ca(II) and Fe(II) did not seem to significantly affect the

rate of U uptake during the first hour of competition (Figure 5 C,D). Finally, Figure 5 E-I shows that, at all the concentrations tested, $MgCl_2$, $MnCl_2$, $ZnSO_4$, Na_2MoO_4 and $CoCl_2$ had almost no effect on U uptake. Again, cell viability was checked throughout the experiment and was largely unaltered regardless of the condition tested (85-99% viability at the end of the experiment, depending on individual cases) (Supplemental Figure 1C), ruling out the possibility that toxic effects of high concentrations of competing metals were primarily responsible for the reduced U uptake rates and accumulation levels. Taken together, our results identified three potential entry pathways for U in yeast; the calcium, copper and iron uptake routes.

S. cerevisiae iron and calcium transport mutants are affected in U uptake

In order to identify metal transporters involved in U uptake in yeast, a set of mutant strains isogenic of BY4742 and affected in the uptake of various metals were assayed for their capacity to accumulate U. The strains *ftr1⊿* and *fet3*Δ are deleted in the genes coding for the permease Ftr1 and the multi-copper ferrous oxidase Fet3, two components of the high-affinity iron Fe(III) uptake system (Stearman et al., 1996). The strain *smf1*Δ is deleted in the gene coding for Smf1 a high-affinity manganese Mn(II) transporter of the Nramp family that can also transport Fe(II), Cu(II) and other divalent metal ions into the cytosol (Chen et al., 1999; Cohen et al., 2000). The strain *ctr1*Δ is deleted in the gene coding for Ctr1 a high-affinity copper transporter that mediates Cu(I) uptake (Dancis et al., 1994). The strains *cch1*Δ and *mid1*Δ are deleted in the genes coding for the two components of the high-affinity plasma membrane voltage-gated calcium channel Cch1, the pore-forming subunit and Mid1, the positive regulatory subunit (Iida et al., 2004; Iida et al., 2017; Iida et al., 2007; Paidhungat and Garrett, 1997). Finally, the stain *cot1*Δ is deleted in the gene coding for Cot1, a transporter induced in iron-deficient yeast that mediates vacuolar accumulation of zinc and cobalt as well as other metals including toxic ones (Conklin et al., 1992; MacDiarmid et al., 2000).

U uptake kinetics in these seven strains are presented in Figure 6. As shown in Figure 6 A,B,C, U uptake was significantly affected in the *ftr1*Δ, *mid1*Δ and *cch1*Δ strains as compared to the wild type. Note that in the *ftr1*Δ strain, the initial rate of U uptake was not altered as compared to the wild type, the inhibitory effect being only visible after 1

h incubation. Some inhibition of U uptake was detected in the *ctr1*Δ and *fet3*Δ mutants but it was not statistically significant (Figure 6 D,E). In contrast, no difference in U uptake was observed in the *smf1*Δ and *cot1*Δ mutants as compared to their wild type counterpart (Figure 6 F,G). Taken together, these data strongly suggest that yeast cells incorporate U at least through the high-affinity iron transporter Ftr1 and the calcium channel Cch1/Mid1.

Finally, the expression from a low copy plasmid, of wild-type copy of *MID1* gene under the control of its own promotor in the corresponding mutant strain restored its capacity to incorporate U to wild-type levels (Figure 7), confirming the role of the Cch1/Mid1 calcium channel in U transport in yeast. We were unable to perform reliable U uptake experiments using the *ftr1*Δ mutant bearing high copy number plasmids encoding Ftr1 and Fet3 proteins. Indeed, the co-expression of these recombinant proteins is controlled by iron deficiency (Stearman et al., 1996) and transformed cells have difficulties to grow properly on synthetic medium deprived of iron, as compared to control cells.

Discussion

In this study, we identified, for the first time, calcium and iron assimilation pathways as important routes for U uptake into a living cell, using *S. cerevisiae* as a model. This was made possible, as discussed below, thanks to the development of an efficient procedure for measuring U transport, under conditions that favor U uptake and that allow to discriminate the uranyl fraction simply adsorbed on the cells from the intracellular fraction.

Living yeast *S. cerevisiae* is able to accumulate U

Over the last four decades, the interactions of the uranyl ion with microorganisms, and particularly the yeast *S. cerevisiae*, have been extensively studied because of their potential use to remediate contaminated waste streams and groundwater (Kolhe et al., 2020; Lu et al., 2013; Nakajima and Tsuruta, 2002; Strandberg et al., 1981). Non-pathogenic and easy obtained at low cost from fermentation industry, *S. cerevisiae* was shown to display a high capacity of U biosorption, a biosorption which consists essentially of adsorption on the cell wall in the experimental conditions used (Chen et

al., 2020; Ohnuki et al., 2005; Volesky and May-Phillips, 1995; Zhang et al., 2020). The most recent investigations proposed a three-step process for biomineralization of U on *S. cerevisiae* cell surface: surface adsorption, amorphous precipitation, and crystallization (Shen et al., 2018; Zheng et al., 2018). U biosorption conditions described so far, using complex media or unbuffered nutrients-free solutions, living or dead cell biomass exposed to elevated U concentrations generally higher than 0.4 mM were optimized for massive U precipitation and/or biomineralization on cell surface. In these conditions, U internalization was rarely evoked and, if so, it was mainly explained by the loss of the cell wall and plasma membrane integrity (Ohnuki et al., 2005; Strandberg et al., 1981; Volesky and May-Phillips, 1995).

In our work, U uptake experiments were performed on living cells exposed to low U concentrations (<100 µM) to preserve cell viability and to limit U precipitation on cell surface, in MES buffer adjusted to pH 5.5, which favors UO_2^{2+}, the bioavailable form of U. This buffer was chosen for its low to negligible metal-chelating propensity (Good et al., 1966) and to prevent pH neutralization of the uptake medium caused by gradual inorganic phosphate and ammonium ions release from inside the yeast cells upon U exposure (Shen et al., 2018; Zheng et al., 2018), minimizing uranyl phosphate precipitation on cell surface. In these conditions, U adsorption on cell surface was extremely rapid, around 80 % of U present in the medium being adsorbed in a few min. This observation compares well with data from literature showing equilibrium reached within 1 to 30 min according to experimental conditions (Faghihian and Peyvandi, 2012; Lu et al., 2013; Nakajima and Tsuruta, 2002; Popa et al., 2003; Volesky and May-Phillips, 1995). To distinguish U externally adsorbed on cell surface from U incorporated within the cell, we used two washings with carbonate, one of the highest affinity ligands for U (Kitano and Oomori, 1971; Poston et al., 1984). In our hands, two washing steps with 10 mM sodium carbonate allowed complete elimination of U adsorbed on cell surface, allowing to unmask U incorporated within the cell. This high washing efficiency was determinant for accurate measurement of uptake kinetics.

Efficient U uptake into *S. cerevisiae* cells depends on the availability of a metabolizable substrate and necessitates a functional respiratory chain

In this work, we showed that an efficient U uptake requires an active metabolism. Indeed, net transport was almost null at 4°C regardless of the presence or absence of externally added glucose in the uptake medium, and low at 30°C in its absence, but it

was highly stimulated in its presence. Interestingly, at low U concentrations (up to 3 µM U) glucose-independent U transport was significant, suggesting passive diffusion contribution to U uptake under these conditions. At 10 µM U, glucose-independent U uptake was almost negligible. At 30°C and in the presence of glucose, U uptake was a saturable process, initial rates of U uptake being saturable at concentrations above 50 µM. In *S. cerevisiae* glucose uptake is mainly performed by facilitated diffusion and is mediated by various uniporters and channels (Boles, 1997; Kruckeberg, 1996; Reifenberger et al., 1997; Wijsman et al., 2019). Since U and glucose are known to form complexes under certain conditions (Steudtner et al., 2010) the hypothesis of a co-transport through hexose transporters could not be excluded at this stage. To test this hypothesis, we used glycerol, which is not able to form complexes with U, as an alternative source of carbon in U uptake experiments. Similar stimulation of U uptake was observed under these conditions, ruling out the possibility of U transport through hexose transporters. The higher rates of U incorporation in the absence of any energy source in uptake medium, when yeasts were initially grown in medium containing glycerol instead of glucose (YG vs YD medium) (Figure 4B), might be explained by some existing internal storage pool of glycerol. In contrast, in yeast exposed to fermentable sugars such as glucose, despite high rates of uptake, little or no sugar can normally be detected within the cell, the glycolytic system removing the sugars as fast as they enter (Klein et al., 2017).

Finally, the use of sodium azide that blocks cell respiration by inhibiting the activity of mitochondrial cytochrome c oxidase-respiratory chain complex (Keilin, 1936; Leary et al., 2002), almost completely abolished U uptake in *S. cerevisiae* cells, whatever the metabolizable substrate source present (glucose or glycerol), demonstrating the importance of a functional respiratory chain in this process. The unaltered viability (cell permeability) of azide-treated cells compared to the control precluded the scenario that the very low U level in these cells resulted from cell death and the release of U to the medium (Supplemental Figure 1B).

Iron, calcium and copper pathways are involved in the absorption of U in *S cerevisiae*

A combination of competition experiments with essential metals and analysis of mutant strains deleted in genes coding for metal importers allowed us to identify calcium, iron and copper pathways as potential routes for U uptake in yeast.

Uptake of U through the calcium assimilation pathway – In this study, we showed that in *S. cerevisiae* calcium and U share a common route for the entry into the cell. U(VI) under its UO_2^{2+} cation form resembles Ca^{2+}. Uranyl coordination properties having some similarities with those of calcium, various calcium-binding proteins from different organisms, including Human, were found to interact strongly with U, among which calmodulin (Brulfert et al., 2016; Le Clainche and Vita, 2006; Pardoux et al., 2012) and osteopontin (Creff et al., 2019; Qi et al., 2014; Safi et al., 2013). In biological systems, U and calcium biosorption relationships are also well documented. In *S cerevisiae*, Ca^{2+} was shown to affect both the initial rate of U biosorption and total amount of U bound to the cell wall (Strandberg et al., 1981). In plants, it was also found that U accumulation in plants was directly related to mobile calcium content in soil (Ratnikov et al., 2020). The interference of U with calcium uptake and homeostasis has been also reported in numerous studies (El Hayek et al., 2018; Moll et al., 2020; Rajabi et al., 2021; Straczek et al., 2009; Tawussi et al., 2017; Vanhoudt et al., 2010). The observed increase in cytoplasmic calcium reported in some cases could represent a cellular defense mechanism in response to the presence of U (White and Broadley, 2003). Within the cell, U(VI) under its UO_2^{2+} cation form can replace Ca^{2+} and Mg^{2+}, which can lead to structural changes to cell membranes, enzyme inactivation, and damage to RNA and DNA (Saenen et al., 2013). Despite all these observations, no direct evidence for the uptake of U by the calcium assimilation pathway was provided so far.

In *S. cerevisiae*, Mid1 (positive regulatory protein) and Cch1 (pore-forming subunit) are the two mandatory components of the high affinity voltage-gated calcium channel (Fischer et al., 1997; Hong et al., 2013; Iida et al., 1994; Iida et al., 2004; Iida et al., 2017; Iida et al., 2007). The Mid1/Cch1 channel becomes activated by various stimuli including depolarization, depletion of secretory calcium (Locke et al., 2000), pheromone stimulation (Paidhungat and Garrett, 1997), hypotonic shock (Batiza et al., 1996), and alkaline stress (Viladevall et al., 2004) or metallic stress (Gardarin et al., 2010). Interestingly, the Mid1/Cch1 calcium channel was previously found to contribute also to Cd^{2+} uptake in yeast (Gardarin et al., 2010).

In our study, we showed that calcium inhibits U uptake in *S. cerevisiae* in a concentration-dependent manner, suggesting a common entry pathway for these two cations. This hypothesis is supported by the fact that UO_2^{2+} and Ca^{2+} are both divalent

cations of similar atomic radius (around 180 pm) and ionic radius (around 80-100 pm). Indeed, the size and shape of the species handled by channels need to match the size of the ion selectivity filter cavity for a proper transport (Gouaux and Mackinnon, 2005). Experimentally, this hypothesis was also supported by the fact that the mutant strains *mid1Δ* and *cch1Δ* had similar phenotypes *i.e.*, low U uptake activity and accumulation, consistent with their contribution to a single functional complex, and that the expression of *MID1* gene into the *mid1Δ* strain restored wild-type levels of U uptake rates (Figure 6B,C). Thus, it is interesting to note the parallel between the kinetics of incorporation of U in calcium import mutants in our study and those for calcium in equivalent mutant strains (Iida et al., 1994; Nakagawa et al., 2007). Together, these observations demonstrated that the main calcium import pathway in yeast is involved in U transport.

The incomplete inhibition of U uptake in *mid1Δ* and *cch1Δ* mutant strains or in wild-type strain challenged with excess calcium suggests that other pathways are involved. A similar conclusion could be drawn for calcium entry in yeast cells (Cui et al., 2009; Iida et al., 1994).

Uptake of U through the iron assimilation pathways – Our study also suggests that U might enter the cell through iron transport systems. As for calcium, U and iron crosstalk is well documented in biological systems, particularly in plants where it was found that U interferes with iron homeostasis (Berthet et al., 2018; Doustaly et al., 2014; Sarthou et al., 2020; Vanhoudt et al., 2011). Also, several ferric iron-binding proteins were found to be able to bind U with high affinity, such as human transferrin, involved in iron transport to the bloodstream (Vidaud et al., 2007) and ferritin, an iron storage protein, from the archea *Purrococus furiosus*, the crayfish *Procambarus clarkia* or the zebrafish *Danio rerio* (Cvetkovic et al., 2010; Eb-Levadoux et al., 2017; Xu et al., 2014).

In the present study, we provided the first experimental evidence that the iron pathway can directly contribute to U uptake in yeast. Indeed, we showed that a mutant strain lacking the ferric iron permease Ftr1 was significantly affected in U uptake. The presence of functional copper-dependent ferrous oxidase Fet3 being required for the maturation of Ftr1 and iron transport across the plasma membrane (De Silva et al., 1995; Hassett et al., 1998a; Stearman et al., 1996) (Figure 8), the rather normal U uptake observed in the mutant strain *fet3Δ* was unexpected (Figure 6E). However, it was shown that yeast can compensate for the lack of Fet3 by overexpressing Fet4, a

low affinity, low specificity Fe(II) ion transporter. This compensation was not observed in the mutant strain *ftr1Δ* (Li and Kaplan, 1998). Thus, in Fet3 defective mutants, U might enter the cell through the Fet4 pathways. In Ftr1 defective mutants, iron enter the cell mainly *via* Smf1, a broad-spectrum low affinity, low saturable divalent cation transporter capable of transporting Mn(II), Zn(II) and Fe(II) (Cohen et al., 2000; Portnoy and Culotta, 2003). Since Smf1 does not seem to be involved in U transport (Figure 6G), this would explain the deficit in U incorporation observed in the *ftr1Δ* mutant. These observations are consistent with the results of competition assays showing that a Fe(II) concentration about 10 times higher than that of Fe(III) was necessary to affect U uptake (Figure 5B,D). Taken together, our results support the idea that *S. cerevisiae* can incorporate U, through the Ftr1/Fet3 high affinity iron transport system.

Uptake of U under copper excess – The negative impact of copper on U uptake by yeast was unexpected. Indeed, the imported form of copper Cu(I) in yeast has very different chemical properties compared to U, notably in terms of protein ligands as deduced from Pearson's (Pearson, 1963) classification. Accordingly, the mutant strain *ctr1Δ* lacking the high affinity Cu(I) transporter Ctr1 was not affected in U uptake (Figure 6D). We can exclude that Ctr3, another high affinity copper transporter, compensate for the lack of Ctr1 since the *Ctr3* gene is inactivated in most laboratory strains by a TY2 transposon, including S288C, the parental strain of BY4247 used in our study (Knight et al., 1996). The inhibitory effect of copper on U uptake might be indirect. For example, it was shown that copper stress induces broad and prolonged rise in cytosolic calcium through vacuolar and endoplasmic reticulum stored calcium release (Jo et al., 2008; Ruta et al., 2016) leading to downregulation of the Mid1/Cch1 calcium influx channel (Hong et al., 2010). Thus, in such a scenario, copper effect on U uptake would be explained by a crosstalk between copper and calcium homeostasis. Similarly, as described above, copper through its interaction with Fet3 is required for high affinity iron transport in yeast (Figure 8) (Dancis et al., 1994; Hassett et al., 1998b). It was shown that exposure to high copper concentrations could indirectly affect the iron transport machinery by compromising copper loading on Fet3 and subsequent translocation of the complex to the plasma membrane (Jo et al., 2008). In this scenario, exposure to copper would indirectly affect U uptake. Finally, at the concentration used in this study, copper slightly affected cell viability (15% of cells were dead after 3h incubation in the presence of 100 µM copper; Supplemental Figure 1C). Thus, we

cannot exclude that inhibition of U uptake by copper was also related to the pleiotropic toxic effects of the latter on yeast metabolism (Shanmuganathan et al., 2004).

Conclusion

In the present work, we have developed an accurate and reliable assay to elucidate U uptake routes in *S. cerevisiae*. Taken together, our data combining energy source requirement experiments, competition assays and mutant analyses, showed that U uptake probably operates through different transport systems, among which the calcium channel Mid1/Cch1 and the iron transport complex Ftr1/Fet3. This is to our knowledge, the first identification of U uptake routes in a living cell. Thus, identifying U-transporters in yeast, represents an important milestone in the fields of radionuclide toxicology and bioremediation. Particularly, our discoveries make possible rapid and systematic *in levuro* functional testing of candidate U transporters of many organisms, regardless of their phylogenetic origins. This can be particularly well suited to identify transporters from multicellular organisms, like higher plants or mammals, prior more complex and time-consuming characterization in their natural context. Validation of yeast-based hypotheses in these organisms would provide new insights into the chemical toxicity of U in higher eukaryotes and is a prerequisite for a future rational management of U in polluted soils, in the food chain, and in human health preservation.

CRediT authorship contribution statement

Revel B.: Methodology, Investigation, Formal analysis. **Catty P.:** Conceptualization; Methodology, Investigation, Formal analysis, Resources, Writing – Review & Editing. **Ravanel S.:** Conceptualization, Formal analysis, Resources, Writing – Review & Editing; **Bourguignon J.:** Conceptualization, Supervision, Methodology, Formal analysis, Resources, Writing – Review & Editing, Funding acquisition. **Alban C.:** Conceptualization, Supervision, Methodology, Investigation, Formal analysis, Resources, Writing – Original draft, Writing – Review & Editing.

Declaration of Competing Interest

The authors declare that they have no known competing financial interests or personal relationships that could have appeared to influence the work reported in this paper.

Acknowledgements

This work was funded by grants from the Agence Nationale de la Recherche (ANR-17-CE34-0007, GreenU Project; ANR-17-EURE-0003, CBH-EUR-GS). The PhD fellowship to B.R. was funded by the CEA (CFR Grant). We gratefully acknowledge Pr Hidetoshi Iida and Dr Robert Stearman for providing us with plasmid constructions used in this study.

Appendix A. Supplementary Material

Table I: Yeast strains used in this study

Strain	Deleted gene	Genotype	Reference
BY4742	WT	MATα *his3Δ1 leu2Δ0 lys2Δ0 ura3Δ0*	Brachmann et al. (1998)
BY*ftr1*Δ	YER145C	MATα *his3Δ1 leu2Δ0 lys2Δ0 ura3Δ0 ftr1*Δ	(Winzeler et al., 1999)
BY*fet3*Δ	YMR058W	MATα *his3Δ1 leu2Δ0 lys2Δ0 ura3Δ0 fet3*Δ	(Winzeler et al., 1999)
BY*mid1*Δ	YNL291C	MATα *his3Δ1 leu2Δ0 lys2Δ0 ura3Δ0 mid1*Δ	(Winzeler et al., 1999)
BY*cch1*Δ	YGR217W	MATα *his3Δ1 leu2Δ0 lys2Δ0 ura3Δ0 cch1*Δ	(Winzeler et al., 1999)
BY*smf1*Δ	YOL122C	MATα *his3Δ1 leu2Δ0 lys2Δ0 ura3Δ0 smf1*Δ	(Winzeler et al., 1999)
BY*cot1*Δ	YOR316C	MATα *his3Δ1 leu2Δ0 lys2Δ0 ura3Δ0 cot1*Δ	(Winzeler et al., 1999)
BY*ctr1*Δ	YPR124W	MATα *his3Δ1 leu2Δ0 lys2Δ0 ura3Δ0 ctr1*Δ	(Winzeler et al., 1999)

Figure legends

Figure 1: Effect of sodium carbonate washes on unmasking U taken up by U-exposed *S. cerevisiae* BY4742 strain cells. Cells grown at late-log phase in YD medium were suspended at a concentration of 2 X 10^8 cells/ml in 10 mM MES, pH 5.5 buffer containing 20 mM glucose, and preincubated for 15 min at 4°C (A) or 30°C (B) before addition of 10 µM uranyl nitrate and further incubation at the above-mentioned temperatures. At the time indicated, 0.5 ml aliquots of the cell suspensions were withdrawn and processed as detailed in the Materials and Methods section. U remaining in the incubation medium after centrifugation of the cell suspensions ("Medium"), in the washing solutions after two washes of pelleted cells with 10 mM sodium carbonate ("First wash" and "Second wash", respectively), and in unwashed and washed cell pellets ("Unwashed cells" and "Washed cells", respectively), was quantified by ICP-MS. Dotted line indicates U remaining in the incubation medium of an acellular control, after centrifugation ("Acellular control"). A result representative of at least three independent experiments is shown. In all experiments, the U recovery profiles were very similar, although the absolute values varied from an experiment to the other.

Figure 2: Stimulation of U uptake rate by glucose in *S. cerevisiae* BY4742 strain. Cells grown at late-log phase in YD medium were suspended at a concentration of 2 X 10^8 cells/ml in 10 mM MES, pH 5.5 buffer containing 20 mM glucose (+ Glucose) or not (- Glucose), and preincubated for 15 min at 4°C or 30°C before addition of 1 µM (A), 3 µM (B) or 10 µM (C) uranyl nitrate and further incubation at the above-mentioned temperatures. At the time indicated, 0.6 ml aliquots of the cell suspensions were taken and processed as detailed in the Materials and Methods section. U present in cell pellets washed twice with 10 mM sodium carbonate was quantified by ICP-MS. Bars = SD; n = 3 independent experiments.

Figure 3: Kinetic parameters determination of U uptake in *S. cerevisiae* BY4742 strain. Cells grown at late-log phase in YD medium were suspended in 10 mM MES, pH 5.5 buffer containing glucose 20 mM, at a concentration of 2 X 10^8 cells/ml and preincubated for 15 min at 30°C before addition of 1 to 70 µM uranyl nitrate and further incubation at 30°C. At appropriate intervals (from 0 to 90 min), aliquots of the cell suspensions were taken and processed as detailed in the Materials and Methods section. U present in cell pellets washed twice with 10 mM sodium carbonate was

quantified by ICP-MS. The initial velocity of U uptake (uptake rate) was then plotted versus U concentration in the reaction medium. Data (dots) were fitted by nonlinear regression to the simple Michaelis-Menten equation (curve) using the Kaleidagraph 4.5 program (Synergy Software, Reading, PA). Bars = SD; n = 2 to 9 independent experiments, for each data point.

Figure 4: Effect of glycerol as an alternate metabolizable substrate to glucose for U uptake in *S. cerevisiae* BY4742 strain. Cells grown at late-log phase in YD (A) or YG (B) medium were suspended at a concentration of 2 X 10^8 cells/ml in 10 mM MES, pH 5.5 buffer containing either 20 mM glucose (+ Glucose) or not (- Glucose) (A) or 3% glycerol (+ Glycerol) or not (- Glycerol) (B) and 10 mM NaN_3 (+ NaN_3) or not (- NaN_3), and preincubated for 15 min at 30°C before addition of 10 µM uranyl nitrate and further incubation at the same temperature. At the time indicated, 0.6 ml aliquots of the cell suspensions were taken and processed as detailed in the Materials and Methods section. U present in cell pellets washed twice with 10 mM sodium carbonate was quantified by ICP-MS. Bars = SD; n = 3 independent experiments. Statistical significance for the comparison of all other conditions versus + Glucose (or + Glycerol) – NaN_3 was determined using a non-parametric Dunnett's test with $P < 0.001$ (*).

Figure 5: Kinetics of U uptake in *S. cerevisiae* BY4742 strain in the presence of potential essential metal competitors. Cells grown at late-log phase in YD medium were suspended at a concentration of 2 X 10^8 cells/ml in 10 mM MES, pH 5.5 buffer containing 20 mM glucose and various concentrations (0 to 1000 µM as indicated) of $CuSO_4$ (A), $FeCl_3$ (B), $CaCl_2$ (C), $FeSO_4$ (D), $MgSO_4$ (E), $MnSO_4$ (F), $ZnSO_4$ (G), Na_2MoO_4 (H) or $CoCl_2$ (I). Cell suspensions were then preincubated for 15 min at 30°C before addition of 10 µM uranyl nitrate and further incubation at the same temperature. At the time indicated, 0.5 ml aliquots of the cell suspensions were taken and processed as detailed in the Materials and Methods section. U present in cell pellets washed twice with 10 mM sodium carbonate was quantified by ICP-MS. Bars = SD when these values exceed the dimensions of the symbols; n = 2 to 4 independent experiments, as indicated.

Figure 6: Kinetics of U uptake in *S. cerevisiae* mutant strains deleted in essential metal transporters. Yeast strains, *ftr1*Δ (A), *mid1*Δ (B), *cch1*Δ (C), *ctr1*Δ (D), *fet3*Δ (E), *cot1*Δ (F), *smf1*Δ (G) and their wild type counterpart (BY4742 strain) were grown at late-log phase in YD medium and then suspended at a concentration of 2 X 10^8 cells/ml in 10

609 mM MES, pH 5.5 buffer containing 20 mM glucose. After a 15 min preincubation at
610 30°C, 10 µM uranyl nitrate was added and cells were further incubated at the same
611 temperature. At the time indicated, 1 ml aliquots of the cell suspensions were taken
612 and processed as detailed in the Materials and Methods section. U present in cell
613 pellets washed twice with 10 mM sodium carbonate was quantified by ICP-MS. Bars =
614 SD; n = 2 to 6 independent experiments, as indicated. Statistical significance (mutant
615 versus wild-type) was determined using a non-parametric Dunnett's test with $P < 0.001$
616 (*).

617 **Figure 7:** Contribution of the calcium channel Cch1/Mid1 to U entry in *S. cerevisiae*
618 BY4742 strain. The yeast *mid1*Δ mutant as well as the wild-type parental BY4742 strain
619 (WT) were transformed with either the empty low copy number plasmid pRS316
620 (vector; WT/vector and *mid1*Δ/vector) or YCpMID1 low copy number plasmid (MID1;
621 *mid1*Δ/MID1) encoding the yeast *MID1* gene under the control of its own promoter.
622 Freshly transformed cells were grown at late-log phase in SD/Ca100, plus amino acids
623 and adenine, minus URA medium and then suspended at a concentration of 2 X 10^8
624 cells/ml in 10 mM MES, pH 5.5 buffer containing 20 mM glucose. After a 15 min
625 preincubation at 30°C, 10 µM uranyl nitrate was added and cells were further incubated
626 at the same temperature. At the time indicated, 1 ml aliquots of the cell suspensions
627 were taken and processed as detailed in the Materials and Methods section. U present
628 in cell pellets washed twice with 10 mM sodium carbonate was quantified by ICP-MS.
629 Error bars = SD; n = 3 independent transformants. Statistical significance was
630 determined using a non-parametric Dunnett's test with $P < 0.001$ (*). NS = not
631 significant.

632 **Figure 8:** Recapitulative scheme of U entry routes in *S. cerevisiae*. Our data support
633 the assertion that the high affinity Mid1/Cch1 calcium channel and the high affinity
634 Ftr1/Fet3 iron transport complex promote U uptake in *S. cerevisiae*. Mid1/Cch1: the
635 high affinity calcium channel; Fre1-3: Fre1, Fre2 and Fre3 reductases reduce the Cu(II)
636 to Cu(I) and Fe(III) to Fe(II); Ctr1: the high affinity Cu(I) transporter; Atx1 chaperonin
637 allows copper supply to the Golgi device in concert with Ccc2 transporter. In the path
638 of secretion, copper is incorporated to various metalloproteins including multi-copper
639 ferrous oxidase Fet3. Once copper incorporated in Fet3, the latter is secreted on the
640 cell surface together with the permease Ftr1 with which Fet3 is physically associated,
641 promoting the transport of iron inside the cell (Ftr1/Fet3, the high affinity iron transport

642 complex). Fet4: low affinity and low specificity Fe(II) ion transporter; Smf1: broad-
643 spectrum low affinity and low saturable divalent cation transporter.

644

645 **Supporting information**

646 **Figure S1:** Viability of *S. cerevisiae* strains in the course of the experiments performed
647 in this study. Viability of yeast cell suspensions (Parental BY4742 wild-type strain and
648 the related isogenic mutant strains) was determined by the fluorescein
649 diacetate/propidium iodide staining method using Yeast viability kit and the automated
650 fluorescence cell counter LUNA-FL (Logos Biosystems) after 4h incubation of cells at
651 30°C in the presence of 20 mM glucose, uranyl nitrate at the indicated concentrations
652 (in µM), and other molecules (as indicated) in 10 mM MES pH 5.5 buffer. The details
653 of growth and assay conditions are given in the Materials and Methods section and in
654 the legend of the figures of the corresponding experiments. (A) Viability of cells from
655 experiments in Figure 3 (Kinetics parameters determination); (B) Viability of cells from
656 experiments in Figure 4A (Effect of sodium azide); (C) Viability of cells from
657 experiments in Figure 5 (Effect of metal competitors). Concentrations of competitors
658 are given in µM from 10 to 1000; (D) Viability of cells from experiments in Figure 6
659 (Mutant strains deleted in essential metal transporters). The results from viable cell
660 counts are shown as relative values (%) as compared to total counted cells. Error bars
661 = SD; n = 2 to 6 independent experiments, as indicated in the legend of the referred
662 figures.

663

664 **References**

665 Batiza, A.F., Schulz, T., Masson, P.H., 1996. Yeast Respond to Hypotonic Shock with a Calcium Pulse. J.
666 Biol. Chem. 271 (38), 23357-23362. https://doi.org/10.1074/jbc.271.38.23357
667 Berthet, S., Villiers, F., Alban, C., Serre, N.B.C., Martin-Laffon, J., Figuet, S., Boisson, A.M., Bligny, R.,
668 Kuntz, M., Finazzi, G., Ravanel, S., Bourguignon, J., 2018. Arabidopsis thaliana plants challenged
669 with uranium reveal new insights into iron and phosphate homeostasis. New Phytologist. 217
670 (2), 657-670. https://doi.org/10.1111/nph.14865
671 Blackwell, K.J., Singleton, I., Tobin, J.M., 1995. Metal cation uptake by yeast: a review. Appl. Microbiol.
672 Biotechnol. 43 (4), 579-584. https://doi.org/10.1007/BF00164757
673 Boles, E., 1997. The molecular genetics of hexose transport in yeasts. FEMS Microbiology Reviews. 21
674 (1), 85-111. https://doi.org/10.1016/s0168-6445(97)00052-1
675 Brachmann, C.B., Davies, A., Cost, G.J., Caputo, E., Li, J., Hieter, P., Boeke, J.D., 1998. Designer deletion
676 strains derived from Saccharomyces cerevisiae S288C: a useful set of strains and plasmids for

677 PCR-mediated gene disruption and other applications. Yeast. 14 (2), 115-132.
678 https://doi.org/10.1002/(SICI)1097-0061(19980130)14:2<115::AID-YEA204>3.0.CO;2-2
679 Brulfert, F., Safi, S., Jeanson, A., Martinez-Baez, E., Roques, J., Berthomieu, C., Solari, P.-L., Sauge-
680 Merle, S., Simoni, É., 2016. Structural Environment and Stability of the Complexes Formed
681 Between Calmodulin and Actinyl Ions. Inorganic Chemistry. 55 (6), 2728-2736.
682 https://doi.org/10.1021/acs.inorgchem.5b02440
683 Chen, C., Hu, J., Wang, J., 2020. Biosorption of uranium by immobilized Saccharomyces cerevisiae. J.
684 Environ. Radioact. 213, 106158-106158. https://doi.org/10.1016/j.jenvrad.2020.106158
685 Chen, X.-Z., Peng, J.-B., Cohen, A., Nelson, H., Nelson, N., Hediger, M.A., 1999. Yeast SMF1 Mediates
686 H-coupled Iron Uptake with Concomitant Uncoupled Cation Currents. J. Biol. Chem. 274 (49),
687 35089-35094.
688 Cohen, A., Nelson, H., Nelson, N., 2000. The family of SMF metal ion transporters in yeast cells. J. Biol.
689 Chem. 275 (43), 33388-33394. https://doi.org/10.1074/jbc.M004611200
690 Conklin, D.S., McMaster, J.A., Culbertson, M.R., Kung, C., 1992. COT1, a gene involved in cobalt
691 accumulation in Saccharomyces cerevisiae. Molecular and Cellular Biology. 12 (9), 3678-3688.
692 https://doi.org/10.1128/mcb.12.9.3678
693 Creff, G., Zurita, C., Jeanson, A., Carle, G., Vidaud, C., Den Auwer, C., 2019. What do we know about
694 actinides-proteins interactions? Radiochimica Acta. 107 (9-11), 993-1009.
695 https://doi.org/10.1515/ract-2019-3120
696 Cui, J., Kaandorp, J.A., Ositelu, O.O., Beaudry, V., Knight, A., Nanfack, Y.F., Cunningham, K.W., 2009.
697 Simulating calcium influx and free calcium concentrations in yeast. Cell calcium. 45 (2), 123-
698 132. https://doi.org/10.1016/j.ceca.2008.07.005
699 Curie, C., Alonso, J.M., Le Jean, M., Ecker, J.R., Briat, J.-F., 2000. Involvement of NRAMP1 from
700 Arabidopsis thaliana in iron transport. Biochemical Journal. 347 (3), 749-749.
701 https://doi.org/10.1042/0264-6021:3470749
702 Cvetkovic, A., Menon, A.L., Thorgersen, M.P., Scott, J.W., Poole, F.L., Jenney, F.E., Lancaster, W.A.,
703 Praissman, J.L., Shanmukh, S., Vaccaro, B.J., Trauger, S.A., Kalisiak, E., Apon, J.V., Siuzdak, G.,
704 Yannone, S.M., Tainer, J.A., Adams, M.W.W., 2010. Microbial metalloproteomes are largely
705 uncharacterized. Nature. 466 (7307), 779-782. https://doi.org/10.1038/nature09265
706 Cyert, M.S., Philpott, C.C., 2013. Regulation of cation balance in Saccharomyces cerevisiae. Genetics.
707 193 (3), 677-713. https://doi.org/10.1534/genetics.112.147207
708 Dancis, A., Yuan, D.S., Haile, D., Askwith, C., Eide, D., Moehle, C., Kaplan, J., Klausner, R.D., 1994.
709 Molecular Characterization of a Copper Transport Protein in S. cerevisiae: An Unexpected Role
710 for Copper in Iron Transport. Cell. 76, 393-402.
711 De Silva, D.M., Askwith, C.C., Eide, D., Kaplan, J., 1995. The FET3 gene product required for high affinity
712 iron transport in yeast is a cell surface ferroxidase. J. Biol. Chem. 270 (3), 1098-1101.
713 https://doi.org/10.1074/jbc.270.3.1098
714 Doustaly, F., Combes, F., Fiévet, J.B., Berthet, S., Hugouvieux, V., Bastien, O., Aranjuelo, I., Leonhardt,
715 N., Rivasseau, C., Carrière, M., Vavasseur, A., Renou, J.-P., Vandenbrouck, Y., Bourguignon, J.,
716 2014. Uranium perturbs signaling and iron uptake response in Arabidopsis thaliana roots.
717 Metallomics. 6 (4), 809-821. https://doi.org/10.1039/c4mt00005f
718 Eb-Levadoux, Y., Frelon, S., Simon, O., Arnaudguilhem, C., Lobinski, R., Mounicou, S., 2017. In vivo
719 identification of potential uranium protein targets in zebrafish ovaries after chronic
720 waterborne exposure. Metallomics. 9 (5), 525-534. https://doi.org/10.1039/c6mt00291a
721 Eide, D., Broderius, M., Fett, J., Guerinot, M.L., 1996. A novel iron-regulated metal transporter from
722 plants identified by functional expression in yeast. Proc. Natl. Acad. Sci. USA. 93 (11), 5624-
723 5628. https://doi.org/10.1073/pnas.93.11.5624
724 Eide, D.J., Clark, S., Nair, T.M., Gehl, M., Gribskov, M., Guerinot, M.L., Harper, J.F., 2005.
725 Characterization of the yeast ionome: a genome-wide analysis of nutrient mineral and trace
726 element homeostasis in Saccharomyces cerevisiae. Genome biology. 6 (9), R77.
727 https://doi.org/10.1186/gb-2005-6-9-r77

El Hayek, E., Torres, C., Rodriguez-Freire, L., Blake, J.M., De Vore, C.L., Brearley, A.J., Spilde, M.N., Cabaniss, S., Ali, A.-M.S., Cerrato, J.M., 2018. Effect of Calcium on the Bioavailability of Dissolved Uranium(VI) in Plant Roots under Circumneutral pH. Environmental Science & Technology. 52 (22), 13089-13098. https://doi.org/10.1021/acs.est.8b02724

Faghihian, H., Peyvandi, S., 2012. Adsorption isotherm for uranyl biosorption by Saccharomyces cerevisiae biomass. Journal of Radioanalytical and Nuclear Chemistry. 293 (2), 463-468. https://doi.org/10.1007/s10967-012-1814-y

Fischer, M., Schnell, N., Chattaway, J., Davies, P., Dixon, G., Sanders, D., 1997. The Saccharomyces cerevisiae CCH1 gene is involved in calcium influx and mating. FEBS Letters. 419 (2-3), 259-262. https://doi.org/10.1016/s0014-5793(97)01466-x

Gao, N., Huang, Z., Liu, H., Hou, J., Liu, X., 2019. Advances on the toxicity of uranium to different organisms. Chemosphere. 237, 124548. https://doi.org/10.1016/j.chemosphere.2019.124548

Gardarin, A., Chédin, S., Lagniel, G., Aude, J.-C., Godat, E., Catty, P., Labarre, J., 2010. Endoplasmic reticulum is a major target of cadmium toxicity in yeast. Molecular Microbiology. 76 (4), 1034-1048. https://doi.org/10.1111/j.1365-2958.2010.07166.x

Good, N.E., Winget, G.D., Winter, W., Connolly, T.N., Izawa, S., Singh, R.M.M., 1966. Hydrogen Ion Buffers for Biological Research *. Biochemistry. 5 (2), 467-477. https://doi.org/10.1021/bi00866a011

Gouaux, E., Mackinnon, R., 2005. Principles of selective ion transport in channels and pumps. Science. 310 (5753), 1461-1465. https://doi.org/10.1126/science.1113666

Hassett, R.F., Romeo, A.M., Kosman, D.J., 1998a. Regulation of high affinity iron uptake in the yeast Saccharomyces cerevisiae. Role of dioxygen and Fe. J. Biol. Chem. 273 (13), 7628-7636. https://doi.org/10.1074/jbc.273.13.7628

Hassett, R.F., Yuan, D.S., Kosman, D.J., 1998b. Spectral and kinetic properties of the Fet3 protein from Saccharomyces cerevisiae, a multinuclear copper ferroxidase enzyme. J. Biol. Chem. 273 (36), 23274-23282. https://doi.org/10.1074/jbc.273.36.23274

Hong, M.-P., Vu, K., Bautos, J., Gelli, A., 2010. Cch1 Restores Intracellular Ca2+ in Fungal Cells during Endoplasmic Reticulum Stress*. J. Biol. Chem. 285 (14), 10951-10958. https://doi.org/https://doi.org/10.1074/jbc.M109.056218

Hong, M.-P., Vu, K., Bautos, J.M., Tham, R., Jamklang, M., Uhrig, J.P., Gelli, A., 2013. Activity of the Calcium Channel Pore Cch1 Is Dependent on a Modulatory Region of the Subunit Mid1 in Cryptococcus neoformans. Eukaryotic Cell. 12 (1), 142-150. https://doi.org/10.1128/ec.00130-12

Iida, H., Nakamura, H., Ono, T., Okumura, A.M.S., Anraku, Y., 1994. MID1, a Novel Saccharomyces cerevisiae Gene Encoding a Plasma Membrane Protein, Is Required for Ca21 Influx and Mating. MOLECULAR AND CELLULAR BIOLOGY. 14 (12), 8259-8271.

Iida, K., Tada, T., Iida, H., 2004. Molecular cloning in yeast by in vivo homologous recombination of the yeast putative α1 subunit of the voltage-gated calcium channel. FEBS Letters. 576 (3), 291-296. https://doi.org/10.1016/j.febslet.2004.09.021

Iida, K., Teng, J., Cho, T., Yoshikawa-Kimura, S., Iida, H., 2017. Post-translational processing and membrane translocation of the yeast regulatory Mid1 subunit of the Cch1/VGCC/NALCN cation channel family. J. Biol. Chem. 292 (50), 20570-20582. https://doi.org/10.1074/jbc.M117.810283

Iida, K., Teng, J., Tada, T., Saka, A., Tamai, M., Izumi-Nakaseko, H., Adachi-Akahane, S., Iida, H., 2007. Essential, Completely Conserved Glycine Residue in the Domain III S2–S3 Linker of Voltage-gated Calcium Channel α 1 Subunits in Yeast and Mammals. J. Biol. Chem. 282 (35), 25659-25667. https://doi.org/10.1074/jbc.M703757200

Jo, W.J., Loguinov, A., Chang, M., Wintz, H., Nislow, C., Arkin, A.P., Giaever, G., Vulpe, C.D., 2008. Identification of Genes Involved in the Toxic Response of Saccharomyces cerevisiae against Iron and Copper Overload by Parallel Analysis of Deletion Mutants. Toxicological Sciences. 101 (1), 140-151. https://doi.org/10.1093/toxsci/kfm226

Keilin, D., 1936. The action of sodium azide on cellular respiration and on some catalytic oxidation reactions. Proceedings of the Royal Society of London. Series B - Biological Sciences. 121 (822), 165-173. https://doi.org/10.1098/rspb.1936.0056

Khare, D., Kumar, R., Acharya, C., 2020. Genomic and functional insights into the adaptation and survival of Chryseobacterium sp. strain PMSZPI in uranium enriched environment. Ecotoxicol. Environ. Saf. 191, 110217-110217. https://doi.org/10.1016/j.ecoenv.2020.110217

Kitano, Y., Oomori, T., 1971. The coprecipitation of uranium with calcium carbonate. Journal of the Oceanographical Society of Japan. 27 (1), 34-42. https://doi.org/10.1007/bf02109313

Klein, M., Swinnen, S., Thevelein, J.M., Nevoigt, E., 2017. Glycerol metabolism and transport in yeast and fungi: established knowledge and ambiguities. Environmental Microbiology. 19 (3), 878-893. https://doi.org/https://doi.org/10.1111/1462-2920.13617

Knight, S.A.B., Labbe, S., Kwon, L.F., Kosman, D.J., Thiele, D.J., 1996. A widespread transposable element masks expression of a yeast copper transport gene. Genes Dev. 10 (15), 1917-1929. https://doi.org/10.1101/gad.10.15.1917

Kolhe, N., Zinjarde, S., Acharya, C., 2020. Impact of uranium exposure on marine yeast, Yarrowia lipolytica: Insights into the yeast strategies to withstand uranium stress. J. Hazard. Mater. 381, 121226. https://doi.org/https://doi.org/10.1016/j.jhazmat.2019.121226

Konietschke, F., Placzek, M., Schaarschmidt, F., Hothorn, L.A., 2015. nparcomp: An R Software Package for Nonparametric Multiple Comparisons and Simultaneous Confidence Intervals. J. Stat. Softw. 64 (9)

Kruckeberg, A.L., 1996. The hexose transporter family of Saccharomyces cerevisiae. Archives of Microbiology. 166 (5), 283-292. https://doi.org/10.1007/s002030050385

Kuo, C.L., Campbell, J.L., 1983. Cloning of Saccharomyces cerevisiae DNA replication genes: isolation of the CDC8 gene and two genes that compensate for the cdc8-1 mutation. Molecular and Cellular Biology. 3 (10), 1730-1737. https://doi.org/10.1128/mcb.3.10.1730

Kushnir, S., 1995. Molecular Characterization of a Putative Arabidopsis thaliana Copper Transporter and Its Yeast Homologue. J. Biol. Chem. 270 (47), 28479-28486. https://doi.org/10.1074/jbc.270.47.28479

Laliberté, J., Labbé, S., 2008. The molecular base for copper uptake and distribution: lessons form yeast. Medicine Sciences (Paris). 24 (3), 277-283. https://doi.org/10.1051/medsci/2008243277

Le Clainche, L., Vita, C., 2006. Selective binding of uranyl cation by a novel calmodulin peptide. Environmental Chemistry Letters. 4 (1), 45-49. https://doi.org/10.1007/s10311-005-0033-y

Leary, S.C., Hill, B.C., Lyons, C.N., Carlson, C.G., Michaud, D., Kraft, C.S., Ko, K., Glerum, D.M., Moyes, C.D., 2002. Chronic Treatment with Azide in Situ Leads to an Irreversible Loss of Cytochrome c Oxidase Activity via Holoenzyme Dissociation*. J. Biol. Chem. 277 (13), 11321-11328. https://doi.org/https://doi.org/10.1074/jbc.M112303200

Li, L., Kaplan, J., 1998. Defects in the Yeast High Affinity Iron Transport System Result in Increased Metal Sensitivity because of the Increased Expression of Transporters with a Broad Transition Metal Specificity. J. Biol. Chem. 273 (35), 22181-22187. https://doi.org/10.1074/jbc.273.35.22181

Locke, E.G., Bonilla, M., Liang, L., Takita, Y., Cunningham, K.W., 2000. A Homolog of Voltage-Gated Ca2+ Channels Stimulated by Depletion of Secretory Ca2+ in Yeast. Molecular and Cellular Biology. 20 (18), 6686-6694. https://doi.org/10.1128/mcb.20.18.6686-6694.2000

Lu, X., Zhou, X.-j., Wang, T.-s., 2013. Mechanism of uranium(VI) uptake by Saccharomyces cerevisiae under environmentally relevant conditions: Batch, HRTEM, and FTIR studies. J. Hazard. Mater. 262, 297-303. https://doi.org/10.1016/j.jhazmat.2013.08.051

MacDiarmid, C.W., Gaither, L.A., Eide, D., 2000. Zinc transporters that regulate vacuolar zinc storage in Saccharomyces cerevisiae. The EMBO J. 19 (12), 2845-2855. https://doi.org/https://doi.org/10.1093/emboj/19.12.2845

Moll, H., Sachs, S., Geipel, G., 2020. Plant cell (Brassica napus) response to europium(III) and uranium(VI) exposure. Environmental science and pollution research international. 27 (25), 32048-32061. https://doi.org/10.1007/s11356-020-09525-2

831 Nakagawa, Y., Katagiri, T., Shinozaki, K., Qi, Z., Tatsumi, H., Furuichi, T., Kishigami, A., Sokabe, M.,
832 Kojima, I., Sato, S., Kato, T., Tabata, S., Iida, K., Terashima, A., Nakano, M., Ikeda, M., Yamanaka,
833 T., Iida, H., 2007. Arabidopsis plasma membrane protein crucial for Ca2+ influx and touch
834 sensing in roots. Proc. Natl. Acad. Sci. USA. 104 (9), 3639-3644.
835 https://doi.org/10.1073/pnas.0607703104
836 Nakajima, A., Tsuruta, T., 2002. Competitive Biosorption of Thorium and Uranium by Actinomycetes.
837 Journal of Nuclear Science and Technology. 39 (sup3), 528-531.
838 https://doi.org/10.1080/00223131.2002.10875523
839 Ohnuki, T., Ozaki, T., Yoshida, T., Sakamoto, F., Kozai, N., Wakai, E., Francis, A.J., Iefuji, H., 2005.
840 Mechanisms of uranium mineralization by the yeast Saccharomyces cerevisiae. Geochimica et
841 Cosmochimica Acta. 69 (22), 5307-5316. https://doi.org/10.1016/j.gca.2005.06.023
842 Paidhungat, M., Garrett, S., 1997. A homolog of mammalian, voltage-gated calcium channels mediates
843 yeast pheromone-stimulated Ca2+ uptake and exacerbates the cdc1(Ts) growth defect.
844 Molecular and Cellular Biology. 17 (11), 6339-6347. https://doi.org/10.1128/mcb.17.11.6339
845 Pardoux, R., Sauge-Merle, S., Lemaire, D., Delangle, P., Guilloreau, L., Adriano, J.-M., Berthomieu, C.,
846 2012. Modulating Uranium Binding Affinity in Engineered Calmodulin EF-Hand Peptides: Effect
847 of Phosphorylation. PLoS ONE. 7 (8), e41922-e41922.
848 https://doi.org/10.1371/journal.pone.0041922
849 Pearson, R.G., 1963. Hard and Soft Acids and Bases. Journal of the American Chemical Society. 85 (22),
850 3533-3539. https://doi.org/10.1021/ja00905a001
851 Popa, K., Cecal, A., Drochioiu, G., Pui, A., Humelnicu, D., 2003. Saccharomyces cerevisiae as uranium
852 bioaccumulating material: The influence of contact time, pH and anion nature. Nukleonika. 48
853 (3), 121-125.
854 Portnoy, M.E., Culotta, V.C., 2003. Iron and Manganese Transporters in Yeast. in, Wiley-VCH Verlag
855 GmbH & Co. KGaA, Weinheim, FRG, pp 447-462.
856 Poston, T.M., Hanf, R.W., Simmons, M.A., 1984. Toxicity of uranium to Daphnia magna. Water, Air, and
857 Soil Pollution. 22 (3), 289-298. https://doi.org/10.1007/bf00159350
858 Qi, L., Basset, C., Averseng, O., Quéméneur, E., Hagège, A., Vidaud, C., 2014. Characterization of UO 2
859 2+ binding to osteopontin, a highly phosphorylated protein: insights into potential
860 mechanisms of uranyl accumulation in bones. Metallomics. 6 (1), 166-176.
861 https://doi.org/10.1039/c3mt00269a
862 R Development Core Team (2011) R: A Language and Environment for Statistical Computing, Vienna,
863 Austria
864 Rajabi, F., Jessat, J., Garimella, J.N., Bok, F., Steudtner, R., Stumpf, T., Sachs, S., 2021. Uranium(VI)
865 toxicity in tobacco BY-2 cell suspension culture - A physiological study. Ecotoxicol. Environ. Saf.
866 211, 111883. https://doi.org/10.1016/j.ecoenv.2020.111883
867 Ratnikov, A.N., Sviridenko, D.G., Popova, G.I., Sanzharova, N.I., Mikailova, R.A., 2020. The Behaviour of
868 Uranium in Soils and the Mechanisms of Its Accumulation by Agricultural Plants. in: Gupta,
869 D.K., Walther, C., eds. Uranium in Plants and the Environment, Springer International
870 Publishing, Cham, pp 113-135.
871 Reifenberger, E., Boles, E., Ciriacy, M., 1997. Kinetic Characterization of Individual Hexose Transporters
872 of Saccharomyces Cerevisiae and their Relation to the Triggering Mechanisms of Glucose
873 Repression. European Journal of Biochemistry. 245 (2), 324-333.
874 https://doi.org/10.1111/j.1432-1033.1997.00324.x
875 Ribera, D., Labrot, F., Tisnerat, G., Narbonne, J.F., 1996. Uranium in the environment: occurrence,
876 transfer, and biological effects. Reviews of environmental contamination and toxicology. 146,
877 53-89. https://doi.org/10.1007/978-1-4613-8478-6_3
878 Ruta, L.L., Popa, C.V., Nicolau, I., Farcasanu, I.C., 2016. Calcium signaling and copper toxicity in
879 Saccharomyces cerevisiae cells. Environmental Science and Pollution Research. 23 (24), 24514-
880 24526. https://doi.org/10.1007/s11356-016-6666-5
881 Saenen, E., Horemans, N., Vanhoudt, N., Vandenhove, H., Biermans, G., Van Hees, M., Wannijn, J.,
882 Vangronsveld, J., Cuypers, A., 2013. Effects of pH on uranium uptake and oxidative stress

883 responses induced in Arabidopsis thaliana. Environ. Toxicol. Chem. 32 (9), 2125-2133.
884 https://doi.org/10.1002/etc.2290
885 Safi, S., Creff, G., Jeanson, A., Qi, L., Basset, C., Roques, J., Solari, P.L., Simoni, E., Vidaud, C., Den Auwer,
886 C., 2013. Osteopontin: A Uranium Phosphorylated Binding-Site Characterization. Chemistry -
887 A European Journal. 19 (34), 11261-11269. https://doi.org/10.1002/chem.201300989
888 Sarthou, M.C.M., Revel, B.H., Villiers, F., Alban, C., Bonnot, T., Gigarel, O., Boisson, A.-M., Ravanel, S.,
889 Bourguignon, J., 2020. Development of a metalloproteomic approach to analyse the response
890 of Arabidopsis cells to uranium stress. Metallomics. 12 (8), 1302-1313.
891 https://doi.org/10.1039/d0mt00092b
892 Schachtman, D.P., Schroeder, J.I., 1994. Structure and transport mechanism of a high-affinity
893 potassium uptake transporter from higher plants. Nature. 370 (6491), 655-658.
894 https://doi.org/10.1038/370655a0
895 Shanmuganathan, A., Avery, S.V., Willetts, S.A., Houghton, J.E., 2004. Copper-induced oxidative stress
896 in Saccharomyces cerevisiae targets enzymes of the glycolytic pathway. FEBS Lett. 556 (1-3),
897 253-259. https://doi.org/10.1016/s0014-5793(03)01428-5
898 Shen, Y., Zheng, X., Wang, X., Wang, T., 2018. The biomineralization process of uranium(VI) by
899 Saccharomyces cerevisiae - transformation from amorphous U(VI) to crystalline chernikovite.
900 Appl. Microbiol. Biotechnol. 102 (9), 4217-4229. https://doi.org/10.1007/s00253-018-8918-4
901 Sikorski, R.S., Hieter, P., 1989. A system of shuttle vectors and yeast host strains designed for efficient
902 manipulation of DNA in Saccharomyces cerevisiae. Genetics. 122 (1), 19-27.
903 Stearman, R., Yuan, D.S., Yamaguchi-Iwai, Y., Klausner, R.D., Dancis, A., 1996. A permease-oxidase
904 complex involved in high-affinity iron uptake in yeast. Science. 271 (5255), 1552-1557.
905 https://doi.org/10.1126/science.271.5255.1552
906 Steudtner, R., Arnold, T., Geipel, G., Bernhard, G., 2010. Fluorescence spectroscopic study on
907 complexation of uranium(VI) by glucose: a comparison of room and low temperature
908 measurements. Journal of Radioanalytical and Nuclear Chemistry. 284 (2), 421-429.
909 https://doi.org/10.1007/s10967-010-0489-5
910 Straczek, A., Wannijn, J., Van Hees, M., Thijs, H., Thiry, Y., 2009. Tolerance of hairy roots of carrots to
911 U chronic exposure in a standardized in vitro device. Environ. Exp. Bot. 65 (1), 82-89.
912 https://doi.org/https://doi.org/10.1016/j.envexpbot.2008.03.004
913 Strandberg, G.W., Shumate, S.E., Parrott, J.R., 1981. Microbial Cells as Biosorbents for Heavy Metals:
914 Accumulation of Uranium by Saccharomyces cerevisiae and Pseudomonas aeruginosa. Applied
915 and Environmental Microbiology. 41 (1), 237-245. https://doi.org/10.1128/aem.41.1.237-
916 245.1981
917 Sun, G.L., Reynolds, E.E., Belcher, A.M., 2019. Designing yeast as plant-like hyperaccumulators for
918 heavy metals. Nature communications. 10 (1), 5080. https://doi.org/10.1038/s41467-019-
919 13093-6
920 Tawussi, F., Walther, C., Gupta, D.K., 2017. Does low uranium concentration generates phytotoxic
921 symptoms in Pisum sativum L. in nutrient medium? Environmental Science and Pollution
922 Research. 24 (28), 22741-22751. https://doi.org/10.1007/s11356-017-0056-5
923 Thomine, S., Wang, R., Ward, J.M., Crawford, N.M., Schroeder, J.I., 2000. Cadmium and iron transport
924 by members of a plant metal transporter family in Arabidopsis with homology to Nramp genes.
925 Proc. Natl. Acad. Sci. USA. 97 (9), 4991-4996. https://doi.org/10.1073/pnas.97.9.4991
926 Van Ho, A., Ward, D.M., Kaplan, J., 2002. Transition metal transport in yeast. Annu. Rev. Microbiol. 56,
927 237-261. https://doi.org/10.1146/annurev.micro.56.012302.160847
928 Vanhoudt, N., Vandenhove, H., Horemans, N., Martinez Bello, D., Van Hees, M., Wannijn, J., Carleer,
929 R., Vangronsveld, J., Cuypers, A., 2011. Uranium induced effects on development and mineral
930 nutrition of Arabidopsis thaliana. Journal of Plant Nutrition. 34 (13), 1940-1956.
931 https://doi.org/10.1080/01904167.2011.610482
932 Vanhoudt, N., Vandenhove, H., Horemans, N., Wannijn, J., Bujanic, A., Vangronsveld, J., Cuypers, A.,
933 2010. Study of oxidative stress related responses induced in Arabidopsis thaliana following

mixed exposure to uranium and cadmium. Plant Physiology and Biochemistry. 48 (10-11), 879-886. https://doi.org/10.1016/j.plaphy.2010.08.005

Vidaud, C., Gourion-Arsiquaud, S., Rollin-Genetet, F., Torne-Celer, C., Plantevin, S., Pible, O., Berthomieu, C., Quéméneur, E., 2007. Structural Consequences of Binding of UO 2 2+ to Apotransferrin: Can This Protein Account for Entry of Uranium into Human Cells? Biochemistry. 46 (8), 2215-2226. https://doi.org/10.1021/bi061945h

Viladevall, L., Serrano, R., Ruiz, A., Domenech, G., Giraldo, J., Barceló, A., Ariño, J., 2004. Characterization of the calcium-mediated response to alkaline stress in Saccharomyces cerevisiae. J. Biol. Chem. 279 (42), 43614-43624. https://doi.org/10.1074/jbc.M403606200

Volesky, B., May-Phillips, H.A., 1995. Biosorption of heavy metals by Saccharomyces cerevisiae. Applied Microbiology and Biotechnology. 42 (5), 797-806. https://doi.org/10.1007/bf00171964

White, C., Gadd, G.M., 1987. The Uptake and Cellular Distribution of Zinc in Saccharomyces cerevisiae. Microbiology. 133 (3), 727-737. https://doi.org/https://doi.org/10.1099/00221287-133-3-727

White, P.J., Broadley, M.R., 2003. Calcium in Plants. Ann. Bot. 92 (4), 487-511. https://doi.org/10.1093/aob/mcg164

Wijsman, M., Świat, M.A., Marques, W.L., Hettinga, J.K., van den Broek, M., Torre Cortés, P.d.l., Mans, R., Pronk, J.T., Daran, J.-M., Daran-Lapujade, P., 2019. A toolkit for rapid CRISPR- Sp Cas9 assisted construction of hexose-transport-deficient Saccharomyces cerevisiae strains. FEMS Yeast Research. 19 (1), 1-12. https://doi.org/10.1093/femsyr/foy107

Winzeler, E.A., Shoemaker, D.D., Astromoff, A., Liang, H., Anderson, K., Andre, B., Bangham, R., Benito, R., Boeke, J.D., Bussey, H., Chu, A.M., Connelly, C., Davis, K., Dietrich, F., Dow, S.W., El Bakkoury, M., Foury, F., Friend, S.H., Gentalen, E., Giaever, G., Hegemann, J.H., Jones, T., Laub, M., Liao, H., Liebundguth, N., Lockhart, D.J., Lucau-Danila, A., Lussier, M., M'Rabet, N., Menard, P., Mittmann, M., Pai, C., Rebischung, C., Revuelta, J.L., Riles, L., Roberts, C.J., Ross-MacDonald, P., Scherens, B., Snyder, M., Sookhai-Mahadeo, S., Storms, R.K., Veronneau, S., Voet, M., Volckaert, G., Ward, T.R., Wysocki, R., Yen, G.S., Yu, K., Zimmermann, K., Philippsen, P., Johnston, M., Davis, R.W., 1999. Functional characterization of the S. cerevisiae genome by gene deletion and parallel analysis. Science. 285 (5429), 901-906. https://doi.org/10.1126/science.285.5429.901

Xu, M., Frelon, S., Simon, O., Lobinski, R., Mounicou, S., 2014. Development of a non-denaturing 2D gel electrophoresis protocol for screening in vivo uranium-protein targets in Procambarus clarkii with laser ablation ICP MS followed by protein identification by HPLC–Orbitrap MS. Talanta. 128, 187-195. https://doi.org/10.1016/j.talanta.2014.04.065

Yamanaka, T., Nakagawa, Y., Mori, K., Nakano, M., Imamura, T., Kataoka, H., Terashima, A., Iida, K., Kojima, I., Katagiri, T., Shinozaki, K., Iida, H., 2010. MCA1 and MCA2 that mediate Ca2+ uptake have distinct and overlapping roles in Arabidopsis. Plant Physiology. 152 (3), 1284-1296. https://doi.org/10.1104/pp.109.147371

Zhang, J., Chen, X., Zhou, J., Luo, X., 2020. Uranium biosorption mechanism model of protonated Saccharomyces cerevisiae. J. Hazard. Mater. 385, 121588-121588. https://doi.org/10.1016/j.jhazmat.2019.121588

Zheng, X.Y., Shen, Y.H., Wang, X.Y., Wang, T.S., 2018. Effect of pH on uranium(VI) biosorption and biomineralization by Saccharomyces cerevisiae. Chemosphere. 203, 109-116. https://doi.org/https://doi.org/10.1016/j.chemosphere.2018.03.165

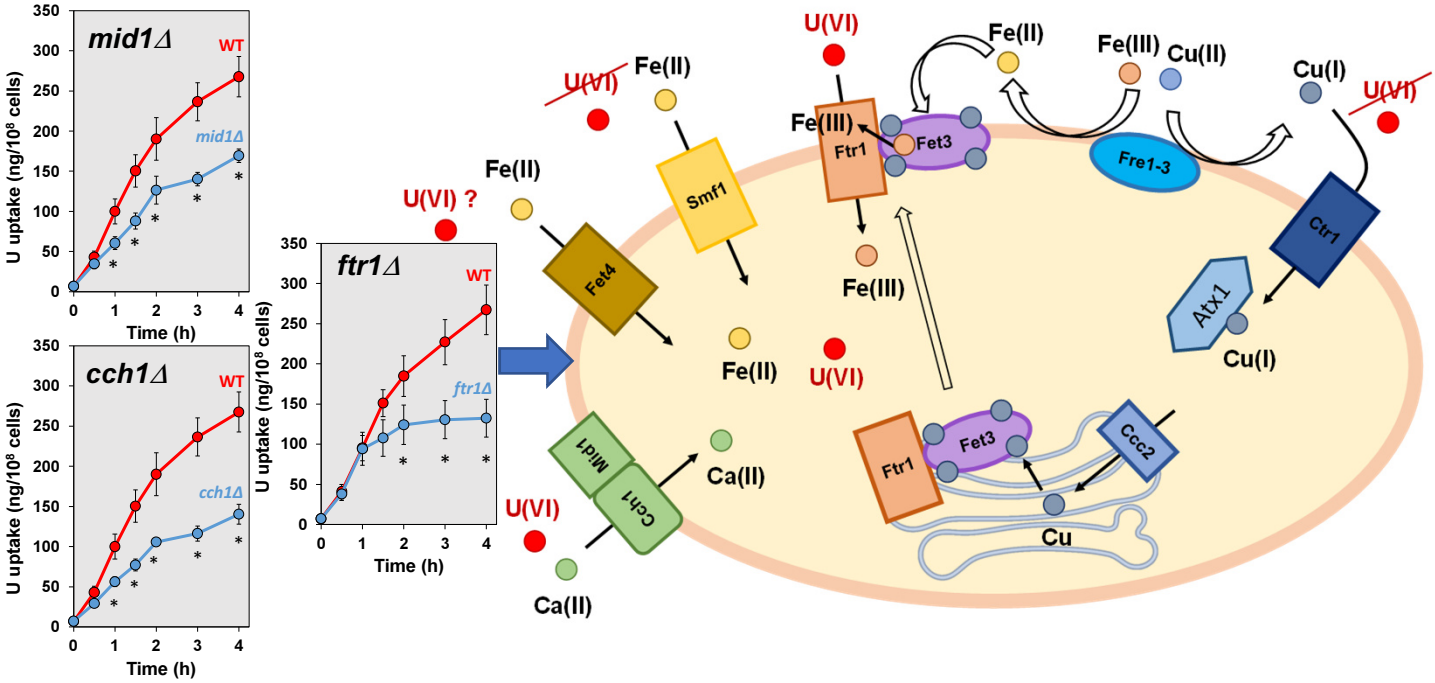

Graphical Abstract

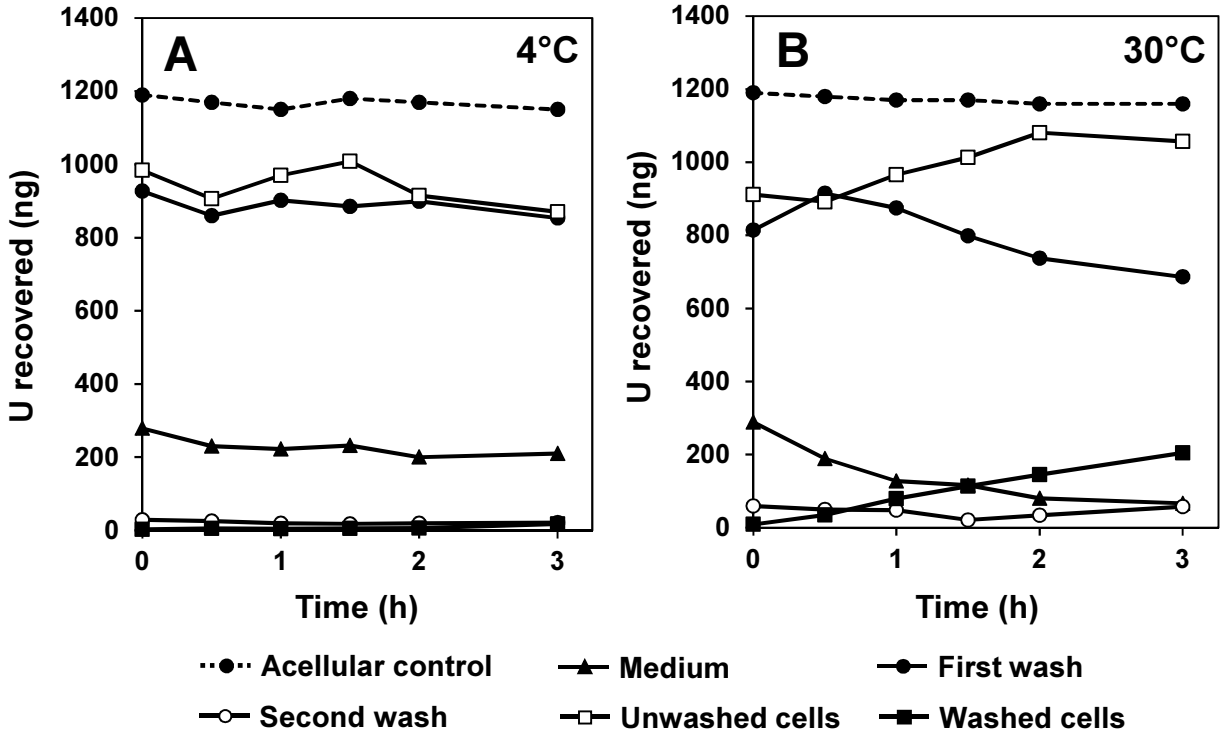

Figure 1: Effect of sodium carbonate washes on unmasking U taken up by U-exposed *S. cerevisiae* BY4742 strain cells. Cells grown at late-log phase in YD medium were suspended at a concentration of 2 X 10^8 cells/ml in 10 mM MES, pH 5.5 buffer containing 20 mM glucose, and preincubated for 15 min at 4°C (A) or 30°C (B) before addition of 10 µM uranyl nitrate and further incubation at the above-mentioned temperatures. At the time indicated, 0.5 ml aliquots of the cell suspensions were withdrawn and processed as detailed in the Materials and Methods section. U remaining in the incubation medium after centrifugation of the cell suspensions ("Medium"), in the washing solutions after two washes of pelleted cells with 10 mM sodium carbonate ("First wash" and "Second wash", respectively), and in unwashed and washed cell pellets ("Unwashed cells" and "Washed cells", respectively), was quantified by ICP-MS. Dotted line indicates U remaining in the incubation medium of an acellular control, after centrifugation ("Acellular control"). A result representative of at least three independent experiments is shown. In all experiments, the U recovery profiles were very similar, although the absolute values varied from an experiment to the other.

Figure 1

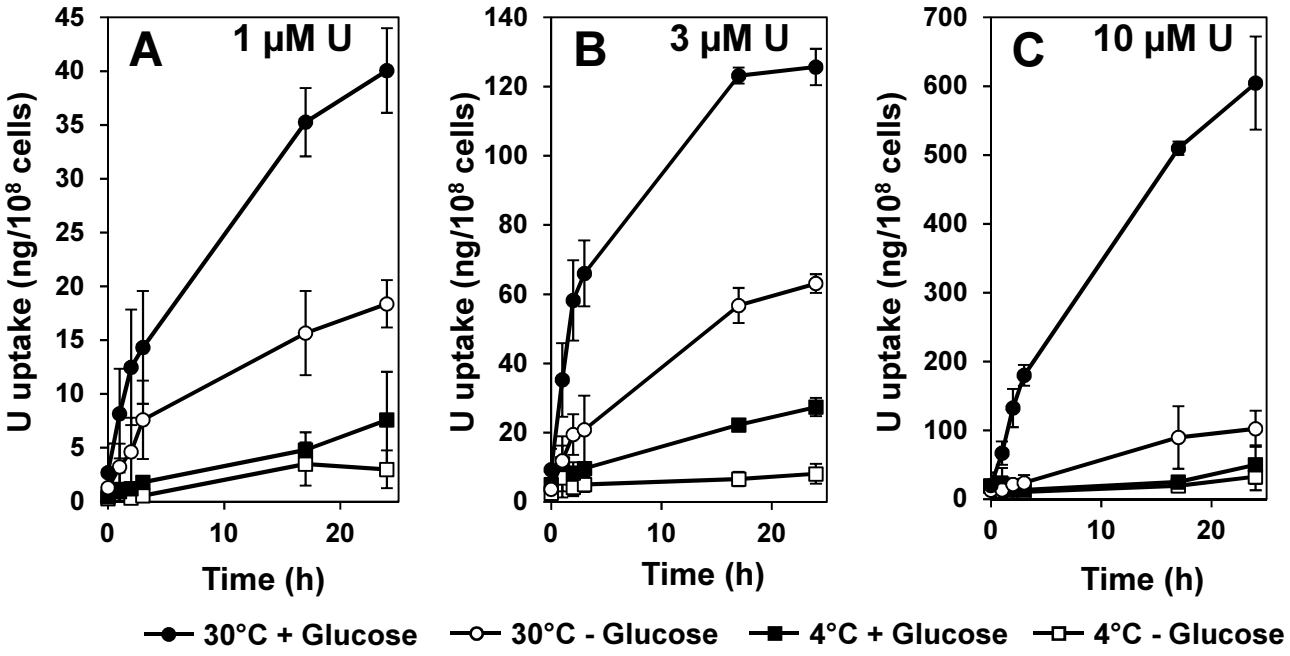

Figure 2: Stimulation of U uptake rate by glucose in *S. cerevisiae* BY4742 strain. Cells grown at late-log phase in YD medium were suspended at a concentration of 2 X 10^8 cells/ml in 10 mM MES, pH 5.5 buffer containing 20 mM glucose (+ Glucose) or not (- Glucose), and preincubated for 15 min at 4°C or 30°C before addition of 1 µM (A), 3 µM (B) or 10 µM (C) uranyl nitrate and further incubation at the above-mentioned temperatures. At the time indicated, 0.6 ml aliquots of the cell suspensions were taken and processed as detailed in the Materials and Methods section. U present in cell pellets washed twice with 10 mM sodium carbonate was quantified by ICP-MS. Bars = SD; n = 3 independent experiments.

Figure 2

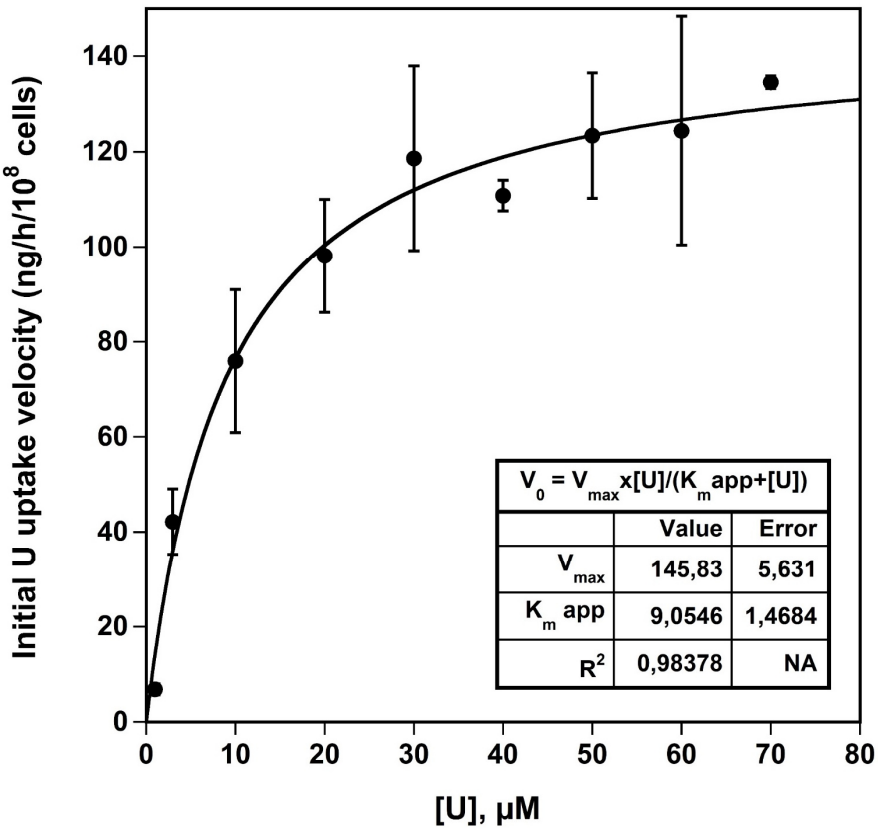

Figure 3: Kinetic parameters determination of U uptake in *S. cerevisiae* BY4742 strain. Cells grown at late-log phase in YD medium were suspended in 10 mM MES, pH 5.5 buffer containing glucose 20 mM, at a concentration of 2 X 10^8 cells/ml and preincubated for 15 min at 30°C before addition of 1 to 70 µM uranyl nitrate and further incubation at 30°C. At appropriate intervals (from 0 to 90 min), aliquots of the cell suspensions were taken and processed as detailed in the Materials and Methods section. U present in cell pellets washed twice with 10 mM sodium carbonate was quantified by ICP-MS. The initial velocity of U uptake (uptake rate) was then plotted versus U concentration in the reaction medium. Data (dots) were fitted by nonlinear regression to the simple Michaelis-Menten equation (curve) using the Kaleidagraph 4.5 program (Synergy Software, Reading, PA). Bars = SD; n = 2 to 9 independent experiments, for each data point.

Figure 3

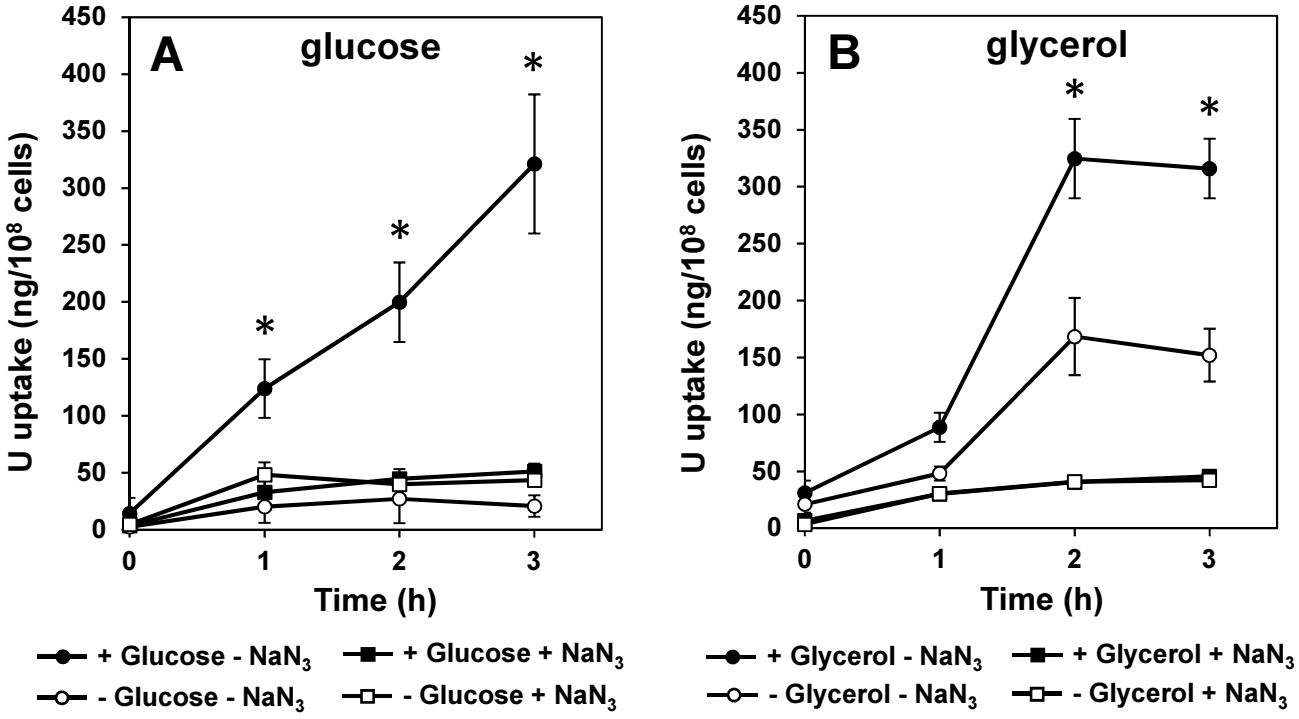

Figure 4: Effect of glycerol as an alternate metabolizable substrate to glucose for U uptake in *S. cerevisiae* BY4742 strain. Cells grown at late-log phase in YD (A) or YG (B) medium were suspended at a concentration of 2 X 10^8 cells/ml in 10 mM MES, pH 5.5 buffer containing either 20 mM glucose (+ Glucose) or not (- Glucose) (A) or 3% glycerol (+ Glycerol) or not (- Glycerol) (B) and 10 mM NaN_3 (+ NaN_3) or not (- NaN_3), and preincubated for 15 min at 30°C before addition of 10 µM uranyl nitrate and further incubation at the same temperature. At the time indicated, 0.6 ml aliquots of the cell suspensions were taken and processed as detailed in the Materials and Methods section. U present in cell pellets washed twice with 10 mM sodium carbonate was quantified by ICP-MS. Bars = SD; n = 3 independent experiments. Statistical significance for the comparison of all other conditions versus + Glucose (or + Glycerol) – NaN_3 was determined using a non-parametric Dunnett's test with $P < 0.001$ (*).

Figure 4

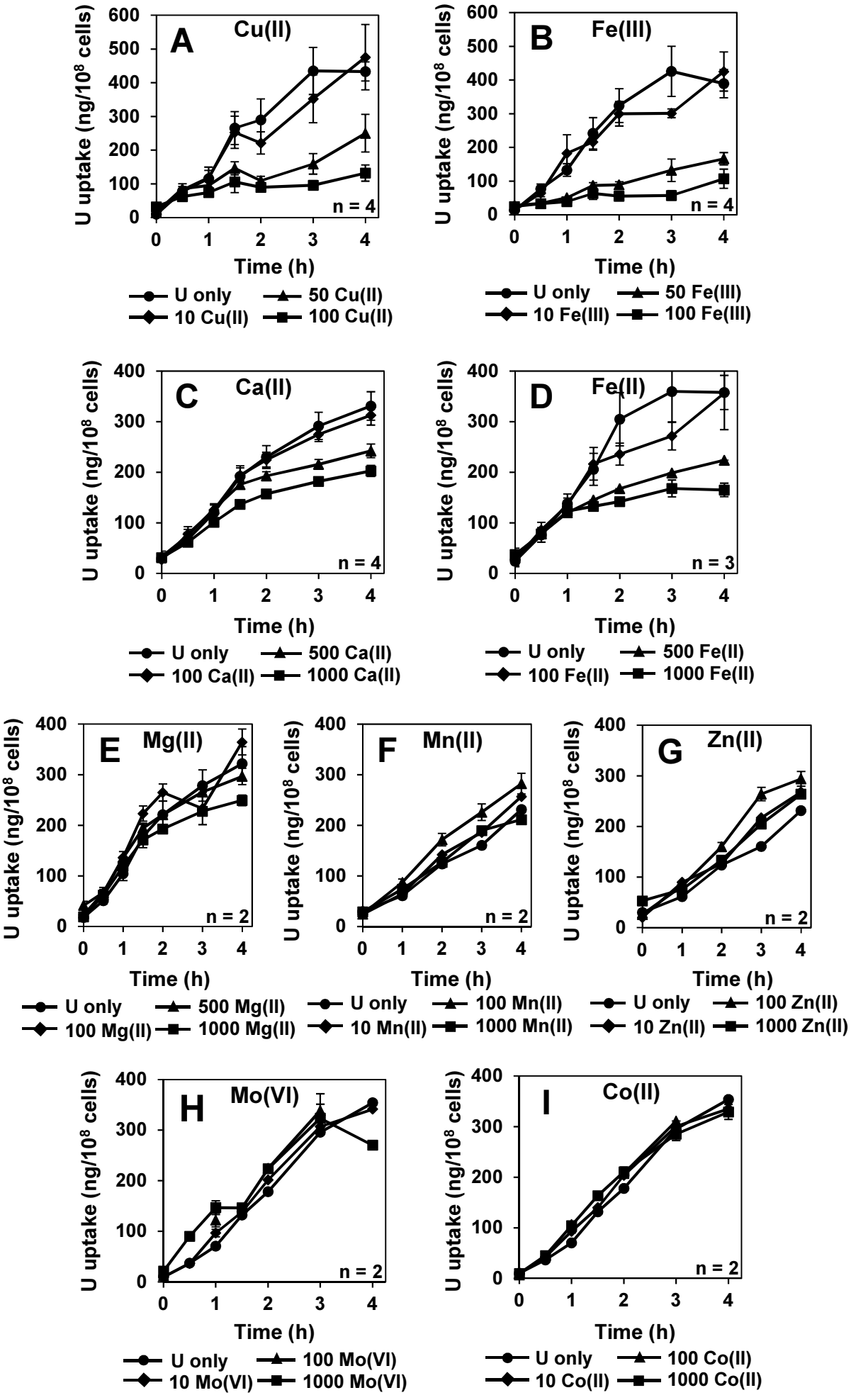

Figure 5 (see legend on the next page)

Figure 5: Kinetics of U uptake in *S. cerevisiae* BY4742 strain in the presence of potential essential metal competitors. Cells grown at late-log phase in YD medium were suspended at a concentration of 2 X 10^8 cells/ml in 10 mM MES, pH 5.5 buffer containing 20 mM glucose and various concentrations (0 to 1000 µM as indicated) of $CuSO_4$ (A), $FeCl_3$ (B), $CaCl_2$ (C), $FeSO_4$ (D), $MgSO_4$ (E), $MnSO_4$ (F), $ZnSO_4$ (G), Na_2MoO_4 (H) or $CoCl_2$ (I). Cell suspensions were then preincubated for 15 min at 30°C before addition of 10 µM uranyl nitrate and further incubation at the same temperature. At the time indicated, 0.5 ml aliquots of the cell suspensions were taken and processed as detailed in the Materials and Methods section. U present in cell pellets washed twice with 10 mM sodium carbonate was quantified by ICP-MS. Bars = SD when these values exceed the dimensions of the symbols; n = 2 to 4 independent experiments, as indicated.

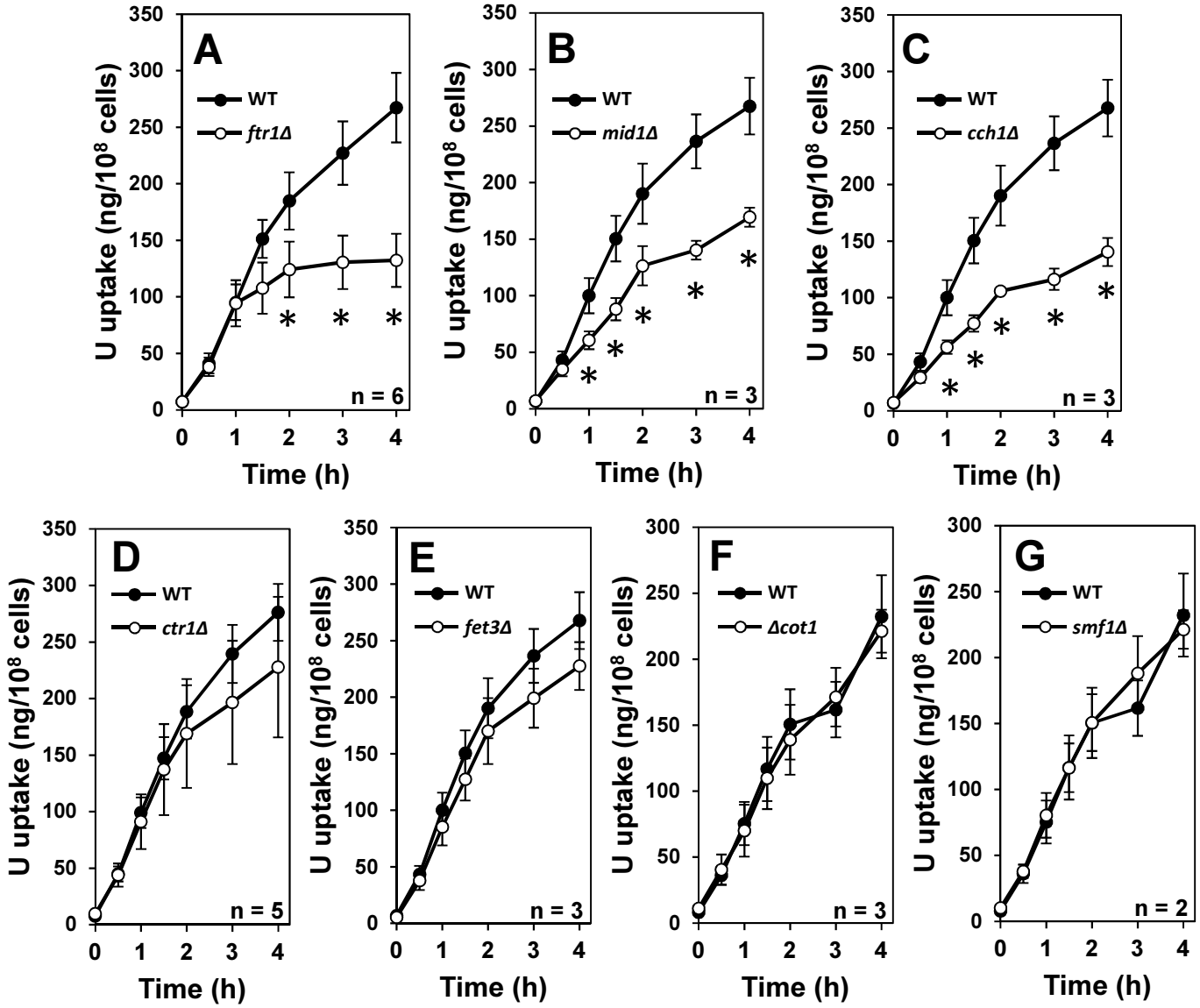

Figure 6: Kinetics of U uptake in *S. cerevisiae* mutant strains deleted in essential metal transporters. Yeast strains, *ftr1*Δ (A), *mid1*Δ (B), *cch1*Δ (C), *ctr1*Δ (D), *fet3*Δ (E), *cot1*Δ (F), *smf1*Δ (G) and their wild type counterpart (BY4742 strain) were grown at late-log phase in YD medium and then suspended at a concentration of 2 X 10^8 cells/ml in 10 mM MES, pH 5.5 buffer containing 20 mM glucose. After a 15 min preincubation at 30°C, 10 µM uranyl nitrate was added and cells were further incubated at the same temperature. At the time indicated, 1 ml aliquots of the cell suspensions were taken and processed as detailed in the Materials and Methods section. U present in cell pellets washed twice with 10 mM sodium carbonate was quantified by ICP-MS. Bars = SD; n = 2 to 6 independent experiments, as indicated. Statistical significance (mutant versus wild-type) was determined using a non-parametric Dunnett's test with $P < 0.001$ (*).

Figure 6

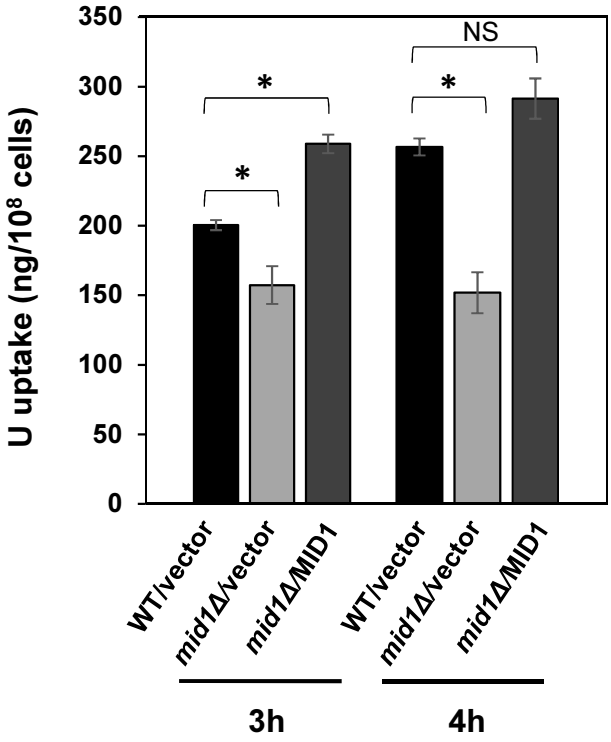

Figure 7: Contribution of the calcium channel Cch1/Mid1 to U entry in *S. cerevisiae* BY4742 strain. The yeast *mid1*Δ mutant as well as the wild-type parental BY4742 strain (WT) were transformed with either the empty low copy number plasmid pRS316 (vector; WT/vector and *mid1Δ*/vector) or YCpMID1 low copy number plasmid (MID1; *mid1Δ*/MID1) encoding the yeast *MID1* gene under the control of its own promoter. Freshly transformed cells were grown at late-log phase in SD/Ca100, plus amino acids and adenine, minus URA medium and then suspended at a concentration of 2 X 10^8 cells/ml in 10 mM MES, pH 5.5 buffer containing 20 mM glucose. After a 15 min preincubation at 30°C, 10 µM uranyl nitrate was added and cells were further incubated at the same temperature. At the time indicated, 1 ml aliquots of the cell suspensions were taken and processed as detailed in the Materials and Methods section. U present in cell pellets washed twice with 10 mM sodium carbonate was quantified by ICP-MS. Error bars = SD; n = 3 independent transformants. Statistical significance was determined using a non-parametric Dunnett's test with $P < 0.001$ (*). NS = not significant.

Figure 7

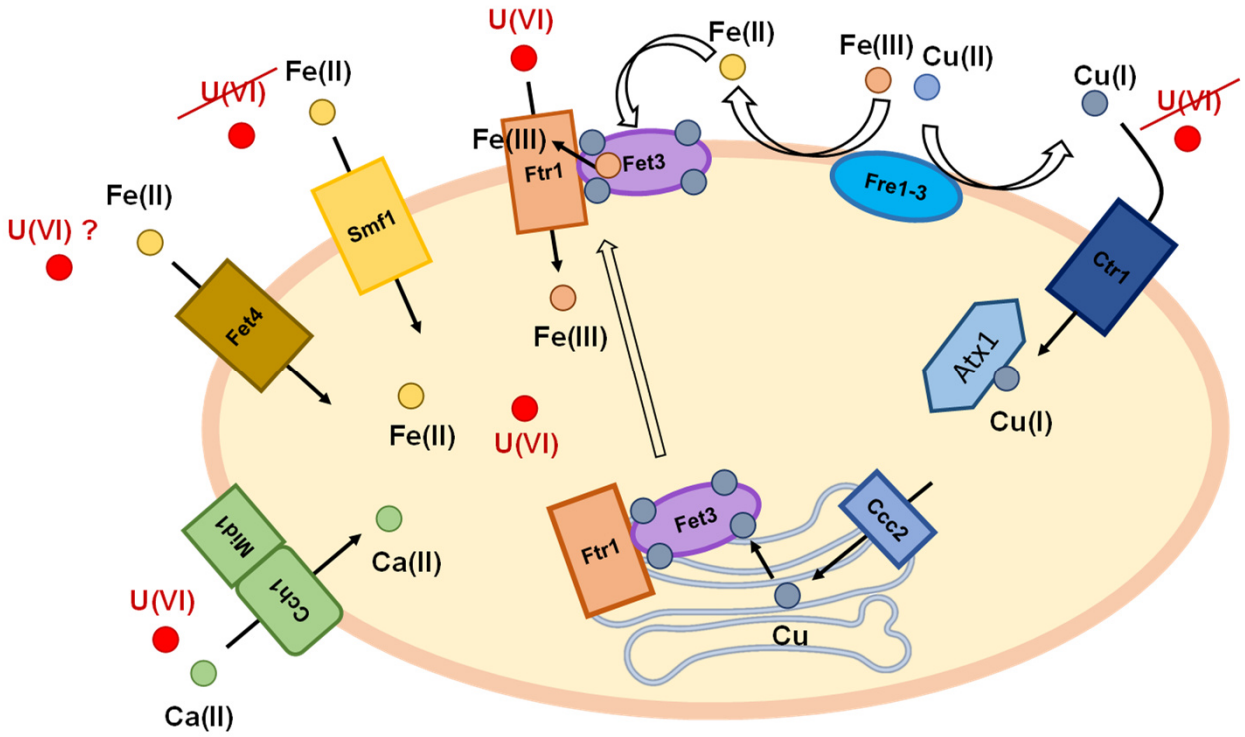

Figure 8: Recapitulative scheme of U entry routes in *S. cerevisiae*. Our data support the assertion that the high affinity Mid1/Cch1 calcium channel and the high affinity Ftr1/Fet3 iron transport complex promote U uptake in *S. cerevisiae*. Mid1/Cch1: the high affinity calcium channel; Fre1-3: Fre1, Fre2 and Fre3 reductases reduce the Cu(II) to Cu(I) and Fe(III) to Fe(II); Ctr1: the high affinity Cu(I) transporter; Atx1 chaperonin allows copper supply to the Golgi device in concert with Ccc2 transporter. In the path of secretion, copper is incorporated to various metalloproteins including multi-copper ferrous oxidase Fet3. Once copper incorporated in Fet3, the latter is secreted on the cell surface together with the permease Ftr1 with which Fet3 is physically associated, promoting the transport of iron inside the cell (Ftr1/Fet3, the high affinity iron transport complex). Fet4: low affinity and low specificity Fe(II) ion transporter; Smf1: broad-spectrum low affinity and low saturable divalent cation transporter.

Figure 8

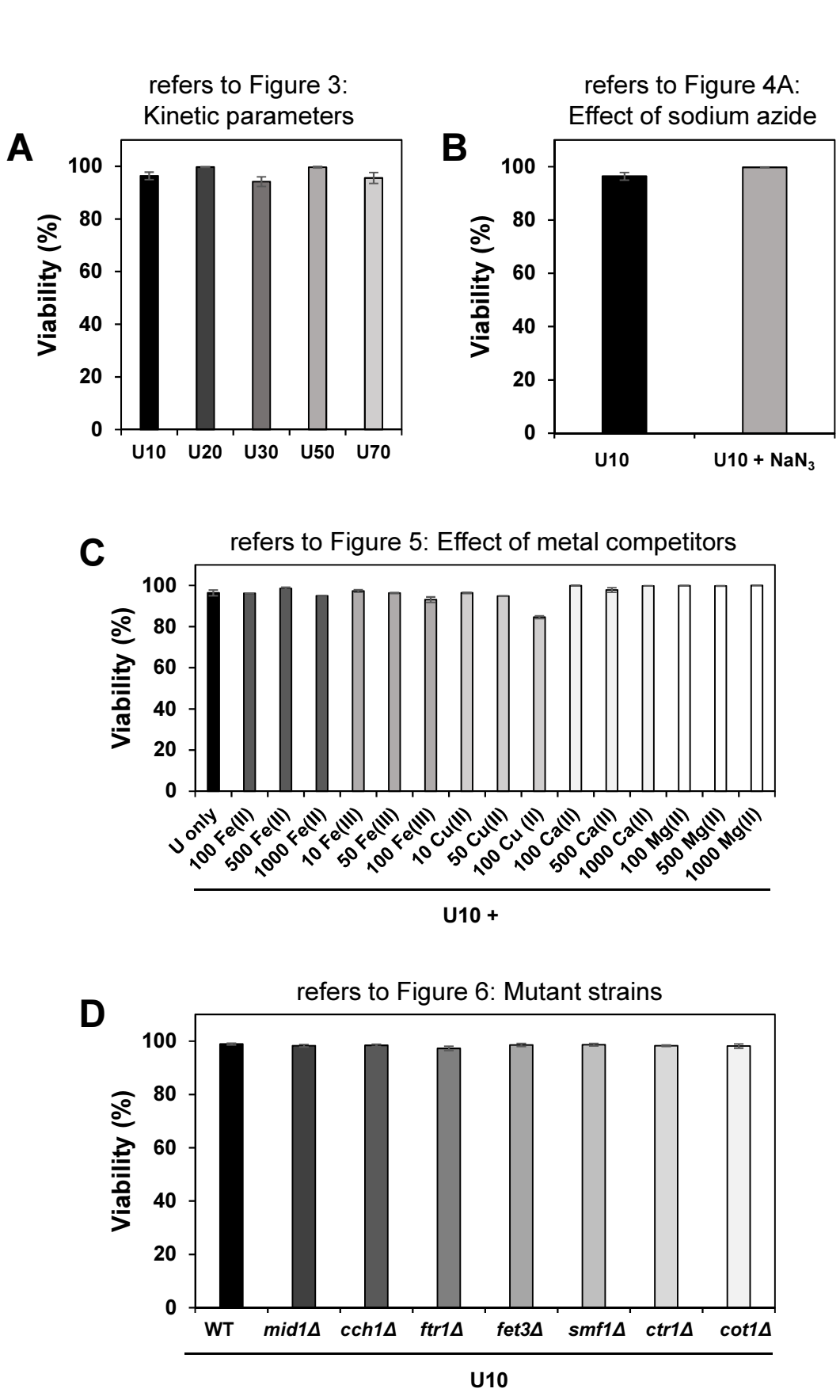

Figure S1 (see legend on the next page)

Figure S1: Viability of *S. cerevisiae* strains in the course of the experiments performed in this study. Viability of yeast cell suspensions (Parental BY4742 wild-type strain and the related isogenic mutant strains) was determined by the fluorescein diacetate/propidium iodide staining method using Yeast viability kit and the automated fluorescence cell counter LUNA-FL (Logos Biosystems) after 4h incubation of cells at 30°C in the presence of 20 mM glucose, uranyl nitrate at the indicated concentrations (in µM), and other molecules (as indicated) in 10 mM MES pH 5.5 buffer. The details of growth and assay conditions are given in the Materials and Methods section and in the legend of the figures of the corresponding experiments. (A) Viability of cells from experiments in Figure 3 (Kinetics parameters determination); (B) Viability of cells from experiments in Figure 4A (Effect of sodium azide); (C) Viability of cells from experiments in Figure 5 (Effect of metal competitors). Concentrations of competitors are given in µM from 10 to 1000; (D) Viability of cells from experiments in Figure 6 (Mutant strains deleted in essential metal transporters). The results from viable cell counts are shown as relative values (%) as compared to total counted cells. Error bars = SD; n = 2 to 6 independent experiments, as indicated in the legend of the referred figures.